Manuscript

Computer Methods in Applied Mechanics and Engineering, Volume 379, June 2021, Article number 113752
DOI: 10.1016/j.cma.2021.113752

Manufacturable insight into modelling and design considerations in fibre–steered composite laminates: state of the art and perspective

B. Sobhani Aragh[a,*], E. Borzabadi Farahani[b], B.X. Xu[a], W.J. Mansur[c]

[a]*Mechanics of Functional Materials Division, Department of Materials Science, Technical University of Darmstadt, 64287 Darmstadt, Germany*
[b]*Institute of Mechanics, Faculty of Mechanical Engineering, Otto von Guericke University Magdeburg, Universitatsplatz 2, 39106 Magdeburg, Germany*
[c]*LAMEMO, Department of Civil Engineering, COPPE, Federal University of Rio de Janeiro, RJ, Brazil*

Abstract

The advent of novel robot–assisted composite manufacturing techniques has enabled steering of fibre paths in the plane of the lamina, leading to the emergence of the so–called variable angle tow (VAT) composite laminates. These laminates, with spatially varying fiber angle orientations, provide the designer with the ability to tailor the point–wise stiffness properties of VAT composites with substantially more efficient structural performance over conventional straight fibre laminates. As the application of fibre–steered composite laminates has reached an unprecedented scale in both academia and industry in recent years, a reflection upon the state–of–the–art advancements in the modelling, design, and analysis of these advanced structures becomes vital for successfully shaping the future landscape. Motivated by the gap and shortcomings in the available review works, in the present paper, we first summarize and discuss underlying fibre placement technologies including tailored fiber placement (TFP), continuous tow shearing (CTS), and automated fibre placement (AFP). Afterwards, mathematical models of reference fibre path in fibre–steering technology will be reviewed, followed by a detailed discussion on the manufacturing limitations and constraints of the AFP process. Then, design considerations in constructing a ply with multiple courses are elaborated, and key techniques to fill the entire layer with several courses are reviewed. This review is then followed by an introduction to the continuity and smoothness of fiber paths. Furthermore, a description on the material and geometric uncertainties is elaborated. Last but not least, the plate and shell laminate theories, which serve as the fundamental core of the modelling and design of VAT composite structures, are discussed.

Keywords: Variable angle tow, Lightweight composite structures, Fibre placement technologies, Modelling and design, Manufacturing constraints, Variable stiffness, Plate and shell laminate theories.

1. Introduction

Fibre–reinforced composites (FRC) have emerged as lightweight structures with widespread use in a myriad of engineering applications. World leaders in 2015 signed the Paris Agreement, aiming to reduce the temperature increase to less than 2^oC above pre–industrial levels [1]. To reach such ambitious goals, countries all over the world will need to strongly reduce CO_2 emissions. The renewable energy technologies, which play a crucial role in a massive reduction of

*Corresponding author
Email address: behnam.sobhaniaragh@tu-darmstadt.de (B. Sobhani Aragh)

Published by Elsevier. This is the Author Accepted Manuscript issued with: Creative Commons Attribution Non-Commercial No Derivatives License (CC:BY:NC:ND 4.0).
The final published version (version of record) is available online at DOI:10.1016/j.cma.2021.113752. Please refer to any applicable publisher terms of use.

List of abbreviations

AFP	Automated fibre placement
APDL	ANSYS parametric design language
ATL	Automated tape laying
ATP	Automated tow placement
BC	Bézier curve
CAD	Computer aided design
CIC	Constant in–plane curvature
CLT	Classical laminate theory
CTS	Continuous tow shearing
CUF	Carrera unified formulation
DFPO	Direct fiber path optimization
ESL	Equivalent–single–layer
FE	Finite element
FEA	Finite element analysis
FN	Fundamental nuclei
FRC	Fibre–reinforced composites
FSDT	First–order shear deformation theories
GDQM	Generalised differential quadrature method
GP	Geodesic path
HSDT	Higher-order shear deformation theory
IGA	Isogeometric analysis
LVFO	Linear variation of fibre orientation
LWT	Layer–wise theory
MCL	Minimum cut length
NLVFO	Non–linear variation of fibre orientation
NURBS	Non–uniform rational B–splines
RBDO	Reliability–based design optimization
RUC	Representative unit cell
TFP	Tailored fiber placement
TSDT	Third–order shear deformation theory
VAT	Variable angle tow
VCQLF	Variable curvature quasi–linear function
VSC	Variable–stiffness composite

CO_2 emissions, are the largest users of FRC [2]. Furthermore, in the aerospace industry in particular, where structural reliability, weight and cost are pivotal, the continuous development and manufacturing of novel structural products is unrelenting. On the other hand, the introduction of astonishing advances in science and technology has motivated novel means of utilizing FRC, such as employing the built–in fiber tailoring competencies in FRC laminates with continuously varying fiber orientation angles, leading to the so–called variable angle tow (VAT) composite laminates. This term is also referred to as variable–stiffness composite (VSC) laminates in the literature. The curvilinear fibre steering capabilities provide the designer with the ability to tailor the point–wise stiffness properties of VAT composites with enlarged design space.

In recent years, VAT composite laminates have evolved from a concept formulated by Olmedo and Gürdal [3] into a proven design technique with sophisticated design frameworks, which incorporate manufacturing, modelling, and analyses, for various types of structural elements. Motivated by the idea of curvilinear fibre–steered composites, curvilinearly stiffened structures have been introduced for the first time by Kapania et al. [4] and gained substantial attention owing to their excellent design flexibility [5, 6, 7]. In particular, curvilinear stiffeners have been demonstrated to be beneficial for cutout reinforcement of thin–walled panels to enhance the strength margins [8]. Hao et al. [9] proposed a novel technique to determine the division of near field and far field, and then performed the optimization of curvilinear stiffeners in the near field. Most recently, a novel layout optimization method was proposed for curvilinearly stiffened panels based on deep

learning–based models [10]. Nevertheless, for the sake of clarity, the present review work will be confined to a specific type of VSC laminates with curvilinear fibre–steered composites.

The prevailing fibre placement technologies to manufacture VAT composite laminates are automated tape laying (ATL), automated fibre placement (AFP), continuous tow shearing (CTS), and tailored fiber placement (TFP). ATL is used to lay up wide prepreg tape on the surface of a mould using a material deposition head while automatically removing the ply backing [11]. The operation principle of AFP is similar to ATL, however, it uses a band of narrow prepreg slices, which are collimated on the head and then delivered together. ATL was introduced in the 1970s and as the technology matured it became the norm in the aeronautic industry for manufacturing comparatively large components with low curvature, such as the wing skins of an airplane. On the contrary, one of the key stimulation behind the advent of AFP, commercially pioneered at the end of the 1980s, was the demand to lay–up onto complex, highly curved moulds, which required tape steering, such as the fuselage of an airplane [12, 13]. Nowadays, AFP plays a crucial role in automated manufacturing of complex aerospace composite components of the new Boeing 787 and Airbus A350 aircrafts. On the other hand, to tackle the process–induced defects of the fibre steering process, such as local fibre wrinkling and tow gaps, using ATL and AFP, Kim et al. [14, 15] at Bristol University has invented the CTS technique, which relied on in–plane shear deformation of partially impregnated tow materials. Using the CTS technique not only substantially simplifies the modelling and design process, but also enhances the quality and performance of VAT composite laminates. As an alternative manufacturing method, TFP [16, 17, 18], invented at the Leibniz Institute of Polymer Research Dresden, is an embroidery–based preform manufacturing process, which permits a flexible orientation of any fiber roving. This technique is high accurate on roving deposition, greatly productive, and enables very small radius of curvature (>5 mm). Furthermore, typical defects in ATL/AFP can be prevented or tailored. In particular, by inducing a slight and smooth overlap, tow gaps may be prevented whilst in–plane fiber waviness can be controlled by adjusting TFP process parameters [19].

Manufacturability constraints are crucial limiting factors that cannot be ignored in the modelling and design of VAT composite laminates, not only to present more realistic and manufacturable design, but also to avoid or reduce process–induced defects, such as fiber discontinuities, breakage, and wrinkling. Several works have investigated the detrimental impacts of those defects on the structural performance for a range of structural properties including strength, buckling resistance, fundamental frequency, etc. The destructive effects of overlap/gap presence on the laminate compression strength of notched and un–notched specimens were assessed experimentally [20]. Local buckling of the slit-tape during the AFP operation has been investigated by Beakou et al. [21] to determine the minimal steering radius for which no tow wrinkling occurs. An experimental work was conducted by Croft et al. [22] to investigate the effect of four principal defect types, including gap, overlap, half gap/overlap and twisted tow, on tensile, compression, and in–plane shear strengths. Fig. 1 shows different segments constituting a VAT composite laminated structure along with relevant manufacturing constraints and design considerations. As can be seen in this figure, minimum cut length (MCL) and minimum steering radius can be defined at the *Tow* and *Course* level, respectively. On the other hand, ply staggering, a technique to prevent gaps and overlaps from regularly occurring at the same location, can be imposed at the *Laminate* level to prevent excessive thickness build–up or resin rich areas.

In order to accomplish the appropriate understanding and ensure reliability and application of fibre–steered composite laminates, modeling and analysis are pivotal steps. To establish an accurate analysis of VAT laminated composites, several theories have been developed and reported in many literature. The literature survey (see Table 1) shows that the vast majority of the works have

been established based on the classical laminate theory (CLT) and the first–order shear deformation theories (FSDT), which both fail to fulfill the interlaminar transverse shear stress continuity at each interface and to explain the so–called zig–zag effect [23]. In particular, the CLT cannot represent properly mechanical behavior of moderately thick to thick laminated composite plates and shells with curvilinear fibre paths. Alternatively, the recourse to more refined structural models, such as higher-order shear deformation theories (HSDT) and layer–wise theories (LWT), is essential. The basis for the improvement and implementation of such higher–order theories can be sought in the works by Carrera [24, 25, 26], where the so–called Carrera unified formulation (CUF) has been presented, which allows whatever refined kinematics for plates and shells to be implemented quickly and easily with no need of an *ad hoc* definition of the finite element (FE) matrices.

Fig. 2a represents a fast growing number of publications and citations in the research field of modelling, design, analysis, and manufacturing of VAT composite laminates over the last fifteen years. As can be seen from Fig. 2a, the total number of publications dramatically increases from 9 in 2005 to 96 in 2019 and the citations on the papers published in 2019 amounts to about 1964. The geographical distribution of the publications in Fig. 2b shows that the USA and western European countries are the home of the vast majority of the research activities in this research field with more than 90% of the published works from these regions. Ghiasi et al. [27, 28] reviewed optimization techniques used for constant– and variable–stiffness design of composite laminates. A review on the buckling, failure and vibrations in laminates reinforced by curvilinear fibres has been presented by Ribeiro et al. [29]. In addition, Gonzalez Lozano et al. [30] provided a review of the design for manufacture of VSC, which has emphasized on the manufacturing limitations of AFP process. Recently, Sabido et al. [31] and Xin et al. [32] presented reviews on the VSC classified only based on the several design criteria, which several aspects of the design and modelling, such as manufacturability, reference fibre path, fundamental theories, etc, have not been discussed in detail. Motivated by the gap and shortcomings in the available review works, in the present review, as the first endeavour, underlying fibre placement technologies including TFP, CTS, and AFP are presented and discussed in detail. Then, mathematical models of reference fibre path in fibre–steering technology will be reviewed, followed by providing a discussion on the manufacturing limitations and constraints of the AFP process. Afterwards, design considerations in constructing a ply with multiple courses are elaborated and key techniques to fill the entire layer with several courses are reviewed. This review is then followed by an introduction to the continuity and smoothness of fiber paths. Furthermore, a description on the material and geometric uncertainties is elaborated. Last but not least, the plate and shell laminate theories, which establish the fundamental core of the modelling and design of VAT composite structures, will be discussed.

2. Fibre placement technologies

Up to now, a number of composite structures have been manufactured with a restricted combination of lay–up configurations (quasi–isotropic, unidirectional, etc.) [33]. This panorama is altering quickly with the prevalent utilization of automated fibre technologies capable of fabricating large composite components with high quality, using continuously varying fibre angles. In the following, the underlying techniques for manufacturing of VAT composite structures are presented and explained.

2.1. Tailored fiber placement (TFP)

As shown in Fig. 3, based on the operation principle of TFP, a single continuous fibre roving can be laid in any directions in a 2–D plane and fixed by a stitching yarn on a flat textile base

material through a double locked stitch with upper and lower thread in a zigzag stitch pattern. The continuous roving is guided based on the design direction by rotating the roving pipe and translation of the base material in two perpendicular directions. TFP is also referred to as dry tow placement in literature [34, 11]. TFP has several advantages over AFP and CTS including the possibility to deposit the fiber roving with small radii, considerable design freedom in terms of the tow path, outstanding out–of–plane mechanical performance, and higher tow deposition speed. Figs. 4a and 4b compare the real and ideal tow deformation according to TFP [35]. Even for the ideal tow deformation, local buckling (waviness) of the fibres inside the curved tow path occurs as a result of the in–plane bending deformation. Nevertheless, in the reality case, a number of process–induced defects take place, as illustrated in Fig. 4a. On one hand, if the tension of supporting the stitching yarn is too high, it causes out–of–plane buckling of the tows. On the other hand, the felt of the substrate allows to some extent stitching yarn movement. Moreover, due to imposing some tension on the tow by the machine head for feeding, the tow is pulled toward the origin of the curvature, leading to resin gaps. It is worth noting that in order to create continuous VAT layers using TFP, the rovings have to be laid with a slight overlap to prevent gaps between them [36].

The vast majority of the literature on the design and modelling of the VAT composite structures manufactured by TFP have been carried out in the Leibniz Institute of Polymer Research Dresden, where the TFP was introduced. There is still need to perform more fundamental and robust numerical modelling and optimisation strategies of the fibre–steered composite parts with accompanying TFP experimental investigations. The capability of TFP preforms as local reinforcements in an open–hole tensile plate was investigated by Gliesche et al. [37], where stresses were computed by finite element analysis (FEA) and validated experimentally with tensile loading tests. The ultimate load was 55% greater for VAT plates manufactured by TFP in comparison with the unidirectional notched plate.

To adequate modeling of continuously varying fibre angles structures manufactured by TFP, a detailed model, which reflects the morphology of TFP including the stitching yarn and the rovings, is required. A numerical study on the impact of a stitching yarn on the mechanical properties of a continuous carbon fiber reinforced plastic layer made by TFP was presented by Uhlig et al. [38]. First, a geometrical analysis of the VAT structure was conducted to determine the dimensions of the roving, resin rich zones, amplitudes of fiber waviness, and the stitching yarn. Afterwards, a parametric FE model of a representative unit cell (RUC), which can be used to create a whole laminate layer, was performed using the ANSYS parametric design language (APDL). The RUC included the base material, split areas for the resin infiltrated roving, and resin rich zones around the upper and lower stitching yarn, as shown in Fig 5. The numerical results were found in good agreement with those obtained from tensile tests according to DIN–EN 527–5 on unidirectional specimens. The RUC approach of this study has provided the basis for determining effective material data for laminates fabricated by TFP.

Zhu et al. [39] studied effects of VAT reinforcements on a notched laminated plate with an open–hole experimentally and numerically. The several factors consisting of the reinforcement types, lay–up configurations, and dimensions were investigated. The FEA, which adopts the 8–node quadrilateral linear shell elements, was performed using the commercial software ANSYS to model the reinforcing mechanism. It has been concluded that the double–sided reinforcement configuration is superior to single–sided or interlayer configurations.

A novel concept for simulation and optimization of open–hole composites with arbitrary lay–up configurations, which relies on the local optimization of both fibre angle and intrinsic thickness build–up simultaneously, has been presented by Bittrich et al. [36]. This framework has been

called direct fiber path optimization (DFPO). The key finding of the work was the local optimization of both fibre angle and thickness at each FE along the base mesh so as to achieve the global optimum. Using similar methodology, notched strength and longitudinal tensile characteristics were experimentally and numerically assessed in un–notched and notched VAT composites [40]. Furthermore, DFPO was employed by Almeida et al. [41] to tailor the stiffness properties of fibre–steered composite cylinders made by TFP for optimizing their specific linear buckling load under axial compression. Fig. 6 compares the buckling modes of conventional and fibre–steered composite cylinders for different lay–up configurations. A rise of 47.9% was achieved for the optimized layout of [VAT$_s$/45/45/VAT$_s$] stacking sequence compared with [0/45/45/0] stacking sequence. As can be seen in this figure, there is a slight loss of symmetry with respect to the shells mid–length, which has been attributed to the non–symmetry of the VAT layers along the z–axis. This characteristics is undesirable in view of structural design purposes. However, these findings are reasonable for the illustration of the proposed methodology, in which the buckling performance is optimized without applying extra constraints to reach a symmetric buckling pattern. In addition, Almeida et al. [42] suggested a methodology to optimize the cross–section of topologically–optimized VAT composite structures for maximizing specific stiffness. In this study, an evolutionary optimization utilizing a genetic algorithm was constructed taking manufacturing characteristics of the TFP process into account by applying constraints to form fiber–steered patterns.

2.2. Automated fibre placement (AFP)

Integrating the advantages of tape laying and filament winding with advanced computer control, AFP has been developed to create high–quality fibre–steered composite structures with tailored properties. AFP, also called automated tow placement (ATP), includes laying down concurrently a large number (up to 32) of fibre tows of 3.175–12.7 mm width to fabricate laminates with continuously varying fibre orientation angles. AFP is a promising technology that provides the designers to tailor and improve the structural performance of composite structures with the wider design space. Since the 1980s AFP has become a comparatively mature operation with high potential for future enhancements and, as a result, vast majority of the literature has been concentrated on the AFP–manufactured composites with arbitrary lay–up configurations, whose orientation varies continuously from point to point. Hence, the reminder of the present review will be dedicated to VAT composites made by AFP, and manufacturing characteristics and limitations of this process are discussed and reviewed in detail.

2.3. Continuous tow shearing (CTS)

The key characteristics of the CTS technique is that the fibre placement head imposes in–plane shear deformation to the tow material fed constantly by fixing the head rotation whereas a single strip of tow is placed [14]. In order to implement shearing capability and avoid the fibre splitting, the CTS technique employs dry tows combined with an *in–situ* impregnation. This mechanism can eradicate tow gaps or overlaps, appeared in the AFP method mainly due to in–plane bending deformation of the tow, because all fibres within a tow can be shifted to have a constant angle through the shifting direction, as shown in Figs. 7a and 7b. In addition, it makes the FEA much easier to be modelled. It is worthwhile noting that based on the CTS method, the coupled variation of the fibre angle and the ply thickness needs to be considered. This can be addressed by retaining the amount of resin for tow impregnation constant [43].

The CTS method can result in a complete shifting method, where all fibres within the tow track an identical path, however, straightforwardly shifted along the designated shifting direction. Figs. 8a and 8b compare the tow arrangements of the VAT composites designed based on AFP

and CTS techniques, respectively. As shown in these figures, using the tow–drop method (See Sec. 5.2) in the conventional AFP method, many fibre discontinuities and tow gaps are produced while the CTS process offers smooth thickness distribution. Consequently, an improvement in the structural strength of the VAT composites is expected [15].

When the tow is sheared, the thickness change is straight associated with the shearing angle. Assuming the constant fibre volume of the tow element, Fig. 9 illustrates the thickness change of the tow element before and after the in–plane shear deformation. The thickness can be easily expressed as

$$t = \frac{t_0}{\sin\theta} \tag{1}$$

where t_0 and θ denote the original tow thickness and the tow shear angle, respectively. The tow angles, which the tow head of the prototype CTS machine can control, is $15^0 \leq \theta \leq 90^0$. Fig. 10 shows a CTS–manufactured VAT composite laminate, which has a thickness variation coupled with shear angle and volume fraction.

The CTS technique is still immature in comparison with ATL, AFP, and TFP technologies that have evolved for more than 20 years. A few studies have been conducted on the design considerations and simulation of the CTS–manufactured fibre–steered composites. A computer aided design (CAD)–based pre–processor has been presented by Kim et al. [44] , which is capable of building ABAQUS FE models of fibre–steered composites considering the manufacturing characteristics of the CTS. It was programmed with AutoLISP language to provide the users with determining curvilinear fibre paths by establishing geometric features in AutoCAD software. By integrating several geometry calculation functions of AutoLISP with geometry creation functions of AutoCAD, it has furnished a convenient way to present an ABAQUS FE model of a VAT composite structure that cannot be formulated mathematically. Nevertheless, further improvement is demanded for its feasibility to 3–D complex surfaces along with the advancement of a head control algorithm dedicated for the CTS process. The buckling behaviour of CTS–manufactured composite panels prismatic fibre variations and symmetric stacking sequences was investigated by Groh et al. [45]. In this study, the fibre angle variations have been constrained to 70^0 since this represents the manufacturing limit of the CTS approach. Dang et al. [46] addressed the two main problems for use of CTS–manufactured VAT in design. Firstly, a methodology for the numerical modelling of 3–D VAT laminates with thickness variation was proposed by a mapping method, which permits a VAT laminate with a reference thickness to be converted to a laminate with spatial coordinate–dependent thickness. Secondly, explicit FE models using bilinear cohesive law–based interface elements and cohesive contacts in Abaqus/Explicit were employed to study the impact and compression after impact behaviour of VAT laminates made by CTS. On the other hand, the post–buckling optimization for the design of VAT layups was performed by Wu et al. [47] using a two–level design framework [48], in which the lamination parameters were employed as the intermediate design variables. The thickness variation owing to both CTS manufacturing of VAT composite laminates and for where it is independent of manufacturing process has been assumed. In other words, stiffness tailoring in the design of the composite structure was conducted by both thickness fibre steering and thickness variation, which was applied to optimize the post–buckling load–carrying capacity of VAT composite plates. This idea was originally taken from the works by Peeters and Abdalla [49, 50] where fiber angle and ply drop optimizations were combined to obtain variable–stiffness variable–thickness composite laminates.

3. Mathematical models of reference fibre path

The definition of the reference fibre path is of high importance in fibre–steering technology, directly affecting product quality and structural performance. Several fibre angle trajectory methods have been proposed, among which linear and non–linear variation of fibre orientation, constant in–plane curvature, geodesic path, and constant angle path have been substantially more emphasized in the literature, as summarized in Table 1.

3.1. Linear variation of fibre orientation

The variable fibre orientation or the fibre trajectories of a VAT lamina are usually represented using mathematical formulas. A linear variation of the fiber orientation along the x coordinate is obtained if the fiber orientation is defined by

$$\varphi(x') = \phi + (T_1 + T_0)\,\frac{|x'|}{d} + T_0 \tag{2}$$

where T_0 denotes the fibre orientation angle at $x' = 0$, T_1 is the fibre orientation angle at $x' = \pm d/2$, and ϕ is the angle of rotation of the fibre path, as illustrated in Fig. 11a. Although the orientation of the fiber angle is changing along a single axis, x', the actual fiber orientation alteration on the $x - y$ plane is a function of both coordinate directions, $\theta = \theta(x, y)$. The representation of a single curvilinear layer is denoted by three independent angles $\phi\,\langle T_0|T_1\rangle$. In order to satisfy the minimum turning radius constraint, the radius of curvature for the reference fibre path can be determined analytically [51].

The linear angle variation path has been widely used in a number of the literature on the VAT composite structures basically due to the concise formulation (See Table 1). Recently, Hao et al. [52] introduced a variable curvature quasi–linear function (VCQLF) by a new governing variable to the linear variation of fibre orientation, motivated by the density function in topology optimization. They reported that comparing the results of fiber path optimization, VCQLF has a higher performance in enhancing the load capacity of VAT shells than that of the conventional definition of the linear angle variation path.

3.2. Non–linear variation of fibre orientation

Overall, non–linear dispersion of fibre orientations on a plane may be characterized by a double series function, for example the Lobatto polynomials. Cubic polynomials for fiber angles have been suggested by Parnas et al. [53], in which coefficients of cubic polynomials were considered as design variables. An expression for defining a curvilinear fibre path employing the normalised Lobatto polynomials has been proposed [54, 55, 56], and it was shown that the non–linear variations result in a better performance than linear variation of fiber orientations. Nevertheless, the coefficients of the Lobatto polynomials were not straightly linked to the fibre angles.

Wu et al. [57, 58] proposed a non–linear dispersion of fibre angles according to Lagrangian polynomials, in which the coefficients of the Lagrangian polynomials are straightly equal to the fibre angles at a set of pre–picked reference points, given by

$$\theta(x, y) = \sum_{m=0}^{M-1}\sum_{n=0}^{N-1} T_{mn} \prod_{m\neq i}\left(\frac{x - x_i}{x_m - x_i}\right) \prod_{n\neq j}\left(\frac{y - y_j}{y_n - y_j}\right) \tag{3}$$

where (x_i, y_j), (x_m, y_n) denote the $x - y$ coordinates of reference points and T_{mn} is fibre angle at a specific reference point (x_m, y_n). Note that the non–linear variation of fibre orientations is based on a set of $M \times N$ pre–picked reference points in the domain, as shown in Fig. 12. It was reported

that non–linear dispersion of the fibre angles leads to nearly a 20% increase in the buckling load compared to linear variation of the fibre angles [57]. Alhajahmad et al. [55] introduced a non–linear function for the fiber orientation angle using Lobatto–Legendre polynomials. It has been concluded that non–linear variations offered more flexibility for the laminate tailoring, thus showing better performance and proving the limitation of using linear variation of fiber orientations. In addition, Zhao and Kapania [59] reported that non–linear variation of fiber path laminates can further increase the buckling loads of stiffened plates for all cases of boundary conditions when compared to those for laminates with the linear variation of fiber paths. In particular, the fiber path can tailor all the in–plane stress resultants distribution into a favorable one to enhance the buckling response significantly. Nonetheless, there is almost no rise in the free vibration fundamental frequency of a simply supported stiffened laminated plate when using the non–linear variation of fiber path.

3.3. Constant in–plane curvature

This definition constitutes based on circular arcs and offers the benefits of creating courses with constant curvature, whose manufacturability with the AFP machine is substantially more convenient than linear/non–linear angle variation paths to check and perform.

The turning radius, which should satisfy the constraint condition $\rho \geq \rho_{\min}$, is defined by

$$\rho = \frac{d}{\sin T_1 - \sin T_0} \tag{4}$$

where $\rho_{\min}$ represents the minimum turning radius of the reference fibre path, as shown in Fig. 11b. Based on the constant in–plane curvature, the angle variation is given by

$$\sin\varphi = \sin T_0 + (\sin T_1 - \sin T_0)\,\frac{x}{d} \tag{5}$$

Mainly, the constant in–plane curvature has been employed in the works [51, 60, 61, 56, 62, 63, 64] dedicated to taking process–induced defects and manufacturing constraints into account. Studying the effect of constant curvature on the optimal VAT laminates, van Campen et al. [62] concluded that introducing a curvature constraint yields the buckling load performance of the VAT plate almost insensitive to the number of layers in the laminate.

3.4. Geodesic path

The geodesic path, having a zero in–plane curvature, has been used as a basis for defining other fibre angle paths since knowledge in the field of geodesic paths for use with filament winding has been already available. In the literature, the geodesic path was only employed to define the fiber orientation path on the conical surface shell [65, 66, 67, 68, 69, 70], as shown in Fig. 13. Fiber angle variation for a geodesic path is expressed by

$$\sin\varphi = \frac{r_0 \sin\bar{T}_0}{r(x)} \tag{6}$$

where $\bar{T}_0$ is the fiber angle at the small radius on the conical shell, which can have a value between -90^0 and 90^0, $r(x)$ denotes the perpendicular distance from the axis of revolution to a point on the shell, and r_0 is smaller radius of the conical shell. Figs. 14a and 14b compare the definition of the fibre angle trajectory based on the geodesic path with those based on the constant angle and constant curvature paths. Blom et al. [68, 70] investigated different path definitions for VAT conical shells, which were used to optimize conical shells for maximum fundamental frequency

whereas manufacturing constraints were taken into account in the process. In this study, although the constant angle path resulted in a constant–stiffness composite laminate, it was used as a baseline for the variable–stiffness designs. Comparing the optimum fundamental frequencies of each fibre path definition for the two different curvature values concluded that for the constant angle path, the value of the maximum curvature has a significant impact on the achievable maximum fundamental frequency. Moreover, it has been observed that the maximum fundamental frequency for the constant curvature path is only moderately affected by the tighter curvature constraint, whereas the frequency of the geodesic path is not affected at all owing to the zero curvature of the fibre path.

3.5. Level set method

The level set method has drawn a lot of attention in moving boundary and front tracking problems in an extensive variety of fields such as interface motion tracking, topology optimization, and image processing. A level set function, such as defined by signed distance function, can be adopted to define the fibre path of a VAT lamina. Considering level set function $\bar{\varphi}(x, y)$ as an implicit function to represent fibre path in x–y plane, the fibre angle at a point is defined as:

$$\varphi = \begin{cases} \arctan\left(-\frac{\frac{\partial\bar{\varphi}(x,y)}{\partial x}}{\frac{\partial\bar{\varphi}(x,y)}{\partial y}}\right), & \text{if } \frac{\partial\bar{\varphi}(x,y)}{\partial y} \neq 0 \\ \frac{\pi}{2}, & \text{if } \frac{\partial\bar{\varphi}(x,y)}{\partial y} = 0 \end{cases} \tag{7}$$

where $\frac{\partial\bar{\varphi}(x,y)}{\partial x}$ and $\frac{\partial\bar{\varphi}(x,y)}{\partial y}$ are the partial derivatives of $\bar{\varphi}$ with respect to x and y. To employ the level set approach to evolve the fibre tow paths when solving the optimization problem, the primary fiber path is assumed by the locations, where the level set function is equal to zero ($\bar{\varphi} = 0$). The other fiber paths at different positions are similarly defined by constant level set function values and, as a result, the level set function characterizes a series of continuous equally spaced parallel fibre paths. A continuous implicit level set function was adopted by Brampton et al. [71] to define the fiber paths throughout the structure. Furthermore, Zhou et al. [72] used a level set function to implicitly describe fibre tow paths, coupled with the solution of an optimization problem. In that work, to maximize the buckling load under thermal loading, sensitivities of thermal buckling eigenvalues with respect to tow paths, i.e. level set values, were derived using the adjoint method.

4. Manufacturing limitations and constraints

AFP process is confronted with a set of restrictions that will influence the manufacturability as well as quality of ideal designs of fibre–steered composite laminates. In order to achieve a manufacturable design, the integration of manufacturing constraints into the modelling, design, and optimization of VAT composite laminates should be accommodated. As a result, herein the most important manufacturing limitations will be introduced [43].

- **Minimum cut length (MCL)**. This length is defined as the distance from the start of the contact point to the tow–cuter in the AFP machine. Consequently, it is not possible to lay a tow in a controlled manner which is shorter than MCL. A manufacturing constraint on MCL, directly implemented in AFP management software, is imposed to guarantee that each tow can be properly laid. It is noteworthy noting that ignoring MCL in the design of VAL laminates may lead to undesirable gaps in the laminate or at ply boundaries, as illustrated in Figs. 15a and 15b. An MCL of 80 mm was considered by Lozano et al. [73] as a manufacturing constant.

- **Gaps and overlaps**. To manufacture a ply, which covers the whole mandrel surface, a number of adjacent courses must be laid, as will be discussed in Sec. 5. Accordingly, gaps and overlaps inevitably may appear during the fibre steering procedure. Generally, when a coverage parameter higher than 0% is chosen in the tow–drop method, a gap and overlap allowance is needed to be considered. As reported by Fayazbakhsh et al. [74] gaps deteriorate both in–plane stiffness and buckling load, while overlaps enhance the structural performance. In particular, the improvement in buckling load arising from the fiber steering declines from 37% to 20% when the impact of gaps is modelled. On the other hand, overlaps rise the improvement in the buckling load to 78%.

- **Minimum turning radius**. This term is the most major manufacturing constraint and must be accounted for in the AFP machine to prevent process–induced defects by the in–plane bending deformation such as local buckling and thickness change of the inner edge of tows. Moreover, if the minimum turning radius is too small, the inner edge of tows undergoes wrinkling, causing imperfections and, as a result, a decline in the strength of the VAT laminate. Nagendra et al. [75] proposed a minimum turning radius of 635 mm.

- **Effective course width**. If the machine is capable of laying n_t tows with a width of t_w, the course width is $C_w = n_t t_w$. The effective course width, W_e, measured along the reference shifting axis (See Fig. 11b), is defined as $W_e = C_w/\cos T_0$. This distance must be constant through the course so as to ensure a full coverage of the ply without gaps or overlaps.

- **Fibre bridging**. When fibres are imposed to tensile forces in the feeding system, they might separate from the mould surface in concave surfaces with high radius.

- **Jagged boundaries**. To prevent large overlaps or gaps in a laminate, a tow–drop method can be applied (Sec. 5.2). As tows are cut normal to the fiber direction, jagged or saw-tooth boundaries will emerge at boundaries that are not perpendicular to this direction. This leads to small gaps, overlaps or a combination of both, which is controlled by a coverage parameter [76].

5. Design considerations in constructing a ply with multiple courses

In order to fill the entire layer with several courses, there are broadly two techniques to construct the other course paths; i.e. *parallel* and *shifted technique* [51]. According to the *parallel method*, each individual fibre path is parallel to the other fibre paths, which alters the tow–orientation in different fibres. The method theoretically results in no gaps or overlaps between tows, leading to a structure of uniform thickness, as illustrated in Fig. 16a. However, this method has not been widely used because the steering radii of each tow are different, which cause violation of the minimum turning radius or maximum allowable curvature. Note that the turning radius decreases by using narrower tow widths, which is less susceptible to wrinkling than wider ones.

On the other hand, in the *shifted method*, by shifting the reference fiber path over a given distance, called the shift distance, along the y'–axis (see Fig. 11a), fibre paths have the same pattern. Rotation of the applicator head of the AFP machine causes a realignment of fibres within a tow parallel to the reference fibre path, which forms overlaps and/or gaps between two adjacent tows, as shown in Fig. 16b. This situation can be more severe when the AFP machine simultaneously places multiple tows to enhance the productivity. Overall, to construct a complete ply, the shifted method can be categorised into the following approaches:

5.1. Tow–overlap technique

Tatting and Gürdal [77] proposed a two–overlap technique, in which a panel allowed the tows to overlap to construct a panel with thickness build–ups that act as "integral stiffeners". Based on this technique, Wu et al. [78] reported that the compressive buckling load of the VAT composite panels increased up to five times than a conventional straight fiber panel. An example of the VAT panel manufactured according to the tow–overlap method is shown in Fig. 17a.

5.2. Tow–drop technique

To avoid large overlaps or gaps in a laminate, thanks to cut–restart capability of the AFP machine, the tow–drop method has been proposed to prevent overlapping zones by cutting the tows when they intersect [51], as shown in Fig. 8a. It leads to a constant thickness structure, which includes small wedge–shape zones free of fibres owing to the dropping of the finite thickness, individual tows. If These small fibre–free regions are prone to form resin rich areas within cure operation, which would be probably hot spots for failure. Fig. 17b illustrates an example of the VAT panel fabricated using the tow–drop method. Fig. 18 illustrates numerical modelling of the tow–drop method used for the simulation of first–ply failure of VAT panels under a tensile load [63, 79]. Considering a configuration for the tow–drop technique with coverage parameter of 0%, a 3–D FE model for a flat tow–steered plate was established by Falco et al. [63]. Their simulations showed how matrix cracking has been affected by discontinuities in the fiber angle between adjacent courses and fiber–free areas resultant from manufacturing effects. In addition, it has been concluded that fiber tensile failure is directly affected by the orientation angles of the fiber, whose distribution depends on the chosen course cutting method: on one side, or on both sides.

Mishra et al. [76] discussed two underlying approaches for cutting strategy of fibre tows. In the conventional cutting strategy, called *single–sided strategy*, at the crossing of two courses, just tows of one of the courses are cut whereas the other course is kept (see Fig. 19a). However, according to the other strategy, called *zipper strategy*, the tows are cut successively, one tow from the course (1), afterwards two tows from the course (2), followed by two tows from the course (1). Comparing Figs. 19a and 19b shows that the intersection line of two courses in the zipper strategy is tracked by fibre tows more smoothly than that in the single–sided strategy.

In the cutting strategy, a so–called coverage parameter [76], between 0 and 100 percent, assesses where tows are being cut and reinitiated, thereby constructing either small wedge–shape gaps or overlaps or a combination of both, as shown in Fig. 20. A coverage parameter of 0 percent implies that a tow is cut as soon as one edge approaches the border of the adjacent course, which causes resin rich areas. At 100 percent coverage parameter, the tow is cut only when the second tow edge passes the border and, as a result, forming a small wedge–shape overlap zones.

5.3. Ply staggering technique

The variation of the thickness in VAT laminates fabricated using the tow–overlap method can be declined by employing a method know as staggering [77, 60]. It encompasses shifting the path of each ply by a small distance, different for each ply. This technique not only helps distributing the tow–drops in case of VAT constant–thickness structures but also results in more uniform tow–overlap structures. The impacts of the tow–drop regions and ply staggering on the stiffness and strength of VAT laminates were theoretically and numerically studied by Blom et al. [61]. In order to spread out irregularities produced by tow–drops, Falco et al. [79] employed the staggering technique and investigated the effect of ply staggering on the un–notched and open–hole VAT laminates tensile strength. Fig. 21 shows the configuration of the open–hole specimen lay–up with

and without staggering. They concluded that ply staggering and 0% coverage parameter play a crucial role in reducing the influence of gaps and overlaps in the VAT laminates.

6. Continuity and smoothness of fiber paths

Generally, there is no guarantee that the fiber angle orientations are continuous and smooth in the traditional FEA. It is because the fibers are discretized at each structural element and are treated as straight fibers. To obtain a smooth distribution of the fiber orientations, ply angles at the nodes rather than at the element were treated as design variables for maximum buckling design of VAT panels [80]. Nevertheless, rapid changes of the optimized fiber angle orientations result in discontinuous fiber paths, which cannot be fabricated in reality. In addition, owing to the non–convexity of the design problem when parametrized using fiber angles, findings are dependent on the starting points. This problem can be addressed using lamination parameters as design variables instead of fiber angles [54, 81, 82, 83]. Setoodeh et al. [54] employed a curve fitting technique to derive continuous fiber angles that leads to a distribution of the lamination parameters near to the optimal dispersion in a least square sense whereas fulfilling the manufacturing constraints. Demir et al. [82, 83] have applied a continuity constrained least–squares, which is obtained by setting the gradient of the fiber angles to zero, to the optimum fiber directions to determine continuous and manufacturable fiber angles. Fig. 22b demonstrates a realistic fiber angle distribution in the context of the manufacturability, before and after the application of LSC method.

An alternative way to present continuous fiber angle orientations that have drawn a lot of attention is using an isogeometric analysis (IGA) formulation based on non–uniform rational B-splines (NURBS). Principally, IGA has been developed with the aim of filling the gap between CAD and FEA, by providing a unified representation of the geometrical design, the computational domain, and the approximation function spaces. The key idea is to employ NURBS, widely used to geometric design in CAD software, as basis functions for the FEA step, providing considerable geometric flexibility and high order continuities at the same time. In particular, geometric design and FEA can be integrated together and, as a result, the element refinement is easily performed by re–indexing the parametric space without altering the geometry or its parameterization. As depicted in Fig. 23, IGA is notably appropriate for the analysis and design of curvilinear fiber paths compared with FEA, since curvilinear fiber path can be exactly represented by the IGA owing to the superior characteristics of NURBS including smoothness, high–order continuity, and reduction of total degree–of–freedom [84].

Hao et al. [85, 84] employed IGA for the buckling analysis of VAT composite panels. Square VAT plates with two types of fiber paths under various loading and boundary conditions were used to investigate the computational efficiency of IGA. It was inferred that IGA has higher computational efficiency that FEA. It is because fiber angle demands to be assigned for each element before FEA is carried out, and accordingly a plenty of CPU time would be spent in FE modeling. However, basis functions generated by NURBS in IGA are employed to represent exact fiber angle paths for arbitrary locations. IGA formulation based on the NURBS along with the Nitsche technique was developed by Khalafi and Fazilati [86, 87] for studying free vibration characteristics of the VAT composite laminated plates. In that work, the cubic NURBS basis functions not only were employed to build the plate's geometry but are also used as the shape functions for FEA field approximations. A Bézier extraction–based IGA model using high–order continuity of NURBS was developed by Shafei et al. [88] for the parametric instability study of anisotropic VAT composite plates. It has been observed that the proposed method can express accurately generalized fiber orientation paths for each ply of the laminate separately. In addition, it was concluded that

it is essential to switch NURBS control mesh to Bézier type so as to achieve the desired accuracy for multi–patch domains.

7. Material and geometric uncertainties

The main source of introducing material and geometric uncertainties [89] in the VAT laminate composites is comparatively complex manufacturing processes owing to the hierarchical nature of these composites. Based on the authors' literature survey, there are few reports on quantifying uncertainties in either material properties or structural performance of VAT composite structures. In the AFP manufacturing process, gaps can be deliberately introduced in some preforms to prevent overlaps, which are resulted from variable tow width. Nonetheless, the presence of variability in the lay–up and gap widths leads to uncertainty in the permeability of the preform. Matveev et al. [90] investigated uncertainty in the geometry of fibre preforms and its impacts on permeability. A perturbation–based stochastic FEM, was adopted by Zhou and Gosling [91] to studied the variability in mechanical performance of VAT composite plates, which have been tailored to have an enhanced buckling performance. They reported that buckling statistics in terms of mean value and standard deviation or coefficient of variation are major functions of uncertainties in fibre tow paths, and should not be ignored. A technique for optimally designing fibre–reinforced symmetrically laminated structures for maximum buckling strength with manufacturing uncertainties in the fibre lay-up orientation has been presented by Walker and Hamilton [92]. The variations in the ply angles were supposed to emanate from the deviations between the manufactured fibre angles and their intended design values. A robust design optimization algorithm was introduced by Zhou et al. [93] for VAT composite structures in the presence of uncertainties in the constituent material properties and applied loads. Uncertainties in the materials properties of the microscopic constituents were considered to fully take into account the hierarchical structure nature of the composite. A probabilistic homogenization approach was employed to propagate uncertainties from micro–scale to macro–scale, establishing a stochastic objective function. It has been concluded that the uncertainties in material properties and applied loads may become a factor that cannot be ignored in the design of VAT composite structures. Hao et al. [94] established an efficient and accurate reliability-based design optimization (RBDO) framework based on IGA for complex engineering problems, in particular for the reliability analysis of a VAT composite panel. It has been inferred that thanks to the advantages of IGA in terms of both efficiency and accuracy, the implementation of IGA will broaden the application scope of RBDO, because the total computational cost becomes affordable for complex engineering problems. Moreover, an RBDO approach has been introduced by Wang et al. [95] and used to design filament–wound cylindrical shells with VAT. The uncertainty in the winding angle was considered in the optimization by means of metamodels constructed using the Kriging method. In that work, stochastic variations of the winding angle were taken into account in the optimization of seven different designs, ranging from constant stiffness to second–order variation of the winding angle with variable thickness.

8. Plate and shell laminate theories

The plate/shell laminate theories constitute the fundamental core of the modelling and design of VAT composite structures. In general, the behavior of multilayered structures can be predicted using either equivalent–single–layer (ESL) theories or three–dimensional (3–D) elasticity theory (or LWT). The ESL theories are resulted from the 3–D elasticity theory by making appropriate assumptions considering the kinematics of deformation or a stress state across the thickness of

the structure. This section presents a comprehensive review on laminate theories developed to predict and understand mechanical behavior of the fibre–steered composite structures. Table 1 summarizes the vast majority of the literature on the design and modelling of VAT composite structures based on the laminate theories.

8.1. Equivalent–single–layer theories

The ESL models may take both shear and normal deformation impacts into account depending on the degree of assumptions. However, all stresses in ESL theories are discontinuous at layer interfaces [96]. Importantly, the transverse stresses at the interface of layers, called interlaminar stresses, do not satisfy the C^0 requirements. The error as a result of discontinuity in interlaminar stresses for thin laminates can be insignificant, however, for thicker laminates, the ESL theories can lead to incorrect results for all stresses, demanding the use of layer–wise theories. The interested readers shall refer to the works by Carrera [97, 98] on the interlaminar stresses and C^0 requirements.

8.1.1. Classical laminated theories

The CLT, as the simplest ESL theory, postulates that normals to the mid–plane before deformation maintain straight and normal to the plane after deformation; that is, transverse shear as well as normal strains are assumed to be negligible with regard to the other strains. Although this assumption results in simple constitutive equations, it is the major drawback of the theory. This theory was first introduced for homogeneous plates, however, later proposed for laminated structures. In spite of major restrictions of the CLT, this theory is still a common approach used in thin VAT composite laminates with arbitrary configuration lay–ups mainly owing to its simplicity with a considerable reduction in the total number of variables and equations, accordingly saving computational time and effort. This can be highlighted when it comes to a optimization procedure.

As the early works in the design and analysis of VAT composites, based on the CLT, Gürdal and Olmedo [99, 3], reported rises up to 50% in the axial stiffness and up to 80% in the critical buckling load of VAT panels compared with conventional straight–fibre composite laminates. The load redistribution from the centre of the domain to the higher–stiffened edge regions was found the underlying reason for these outstanding results.

Wu et al. [57, 100] studied pre–buckling, buckling, and post–buckling analyses of VAT thin plates based on the CLT using a Rayleigh–Ritz approach. It was inferred that the approach are applicable to mixed boundary conditions and were found to be computationally less expensive compared to FEM. In addition, the same authors [58] using a genetic algorithm showed that the optimal fiber paths for improving buckling load decrease the out–of–plane post–buckling displacement. The aeroelastic behaviour of a simple rectangular unswept VAT wing combined with modified strip aerodynamics theory was investigated by Stodieck [101]. Hellinger–Reissner mixed variational principle in conjunction with Lagrange multipliers was employed by Groh et al. [102] to model transverse shear stresses, in bending of VAT laminated plates using the generalised differential quadrature method (GDQM) [103, 104, 105]. The governing equations have been derived based on the CLT with retaining simplifying kinematical assumptions. However, to address the key limitations of the theory, such as shear locking or membrane locking [106, 107], through–the–thickness normal and shear stresses were derived in an exact manner, by virtu of a stress–based approach, integrating the Cauchy's equations governing the elastic continuum. In this way, the continuity of transverse shear stresses at layer interfaces can be assured by solving for the constants of integration. It has been reported that the discrepancies of up to 43% compared to CLT for

span–to–thickness ratios of 10:1 underline the demand for accounting for transverse shear impacts in modelling the flexural behaviour of VAT panels.

Vescovini et al. [108] employed a Koiter's perturbation method along with a mixed variational approach for analyzing the post–buckling behaviour of VAT thin plates according to CLT. A Koiter–Newton method was extended to non–linear buckling analysis, including the pre– and post–buckling stage, of VAT plates based on the CLT [109]. Linear static and buckling analyses of arbitrary cross–section VAT cylinders based on the CLT were established by Khani et al. [110] and a two–step optimisation framework was employed to separate the theoretical and manufacturing issues in design. An analytical model with a CLT–based Rayleigh–Ritz approach was developed by Chen et al. [111] to investigate the characteristics of the buckling response of VAT composite plates with a through–the–width or an embedded rectangular delamination. It was concluded that the buckling strength of composite plates with a delamination can be significantly improved by particular VAT configurations. Raju et al. [112] developed a numerical methodology based on the GDQM for buckling analysis of VAT panels modelled using CLT.

8.1.2. Shear deformation theories

A number of theories have been introduced to model thicker laminated composite plates to account for the transfer shear impact. Majority of those theories are developments of the conventional theories suggested by Reissner [113], Hencky [114], and Mindlin [115], which are referred to as the shear deformation plate theories. The Hencky–Mindlin model is known as the FSDT, which takes the shear deformation effect into account in the form a linear variation of the in–plane displacements through the thickness. Based on the FSDT, transverse straight lines before deformation remain straight after deformation, however, they are no longer normal to the mid–plane after deformation. It is worthwhile noting that the Reissner theory is not analogous to the Mindlin theory, as in many works misleading phrases such as "Reissner–Mindlin plates" and "FSDT of Reissner" have been used, as explained in detail in the works by Wang et al. [116] and Thai et al. [117]. The buckling analysis of complex VAT shells was performed by Hao et al. [52] based on the FSDT and rotation boundary conditions were imposed explicitly. Principally, because of the complexity of shells, the curvature of local surface changes so keenly, which the shear deformation through thickness cannot be neglected. Most recently, Antunes et al. [118] compared the natural frequencies and mode shapes of vibration of a VAT plate obtained by experimental modal analysis with the ones resulting from the numerical modelling based on the CLT and FSDT for three types of boundary conditions including one edge clamped and the other three free, two opposite edges clamped and the other two free, and four edges free. In the four edges free case, both CLT and FSDT models provided natural frequencies and mode shapes reasonably close to the experimental ones. Furthermore, it was reported that the consideration of translational and torsional springs distributed along the boundaries led to mathematical models that predicted the experimentally obtained natural frequencies and natural mode shapes of vibration with much better accuracy.

The limitations of the CLT and FSDT have stimulated several HSDT, among which, including the second–order shear deformation formulation of Whitney and Sun [119] and the third–order shear deformation theory (TSDT) of Lo et al. [120] with 11 unknowns, Kant [121] with six unknowns, Bhimaraddi and Stevens [122] with five unknowns, Hanna and Leissa [123] with four unknowns, the TSDT of Reddy [124] with five unknowns is the most broadly adopted model in the study of shells due to its high efficiency and simplicity [125]. The HSDT are based on an assumption of non–linear stress variation through the thickness. It is worthy mentioning that the displacement field of the TSDT of Reddy is equivalent to that of Levinson theory [126]. Nevertheless, the equations of motion of two theories are different from each other. It is because

Levinson employed the equilibrium equations of the FSDT, which are variationally inconsistent with those resulted from the variational approach by Reddy. Taking both the CLT and TSDT into account, static bending, buckling, and free vibration of a moderately–thick laminated VAT plate with embedded gaps and overlaps have been studied by Akbarzadeh et al. [127]. For very thin plates with continuously variable fibre angle distributions, both the CLT and TSDT led to very close results. But, for moderately–thick plates with length–to–thickness ratio of 10, substantial discrepancies occurred between the ESL theories predictions. In particular, differences up to 23%, 33%, and 15% have been observed for the maximum out–of–plane deflection, critical buckling load, and fundamental frequency, respectively. Furthermore, this work has highlighted that the discrepancy between the ESL theories depends on the amount and type of the embedded defects. For the case of the model incorporating the effects of overlaps, there was a discrepancy up to 26% in the maximum deflection calculated with the CLT and TSDT. This discrepancy was about 22% by considering the effects of gaps in the model.

8.2. Layer–wise theories

Although ESL theories can explain transverse shear and normal strains, encompassing transverse warping of cross section, the model is "kinematically homogeneous" in the manner that the kinematics are insensitive to each single layer. If in–depth response of each single layer is needed and if considerable variations in displacements gradients between layers occur, these theories will demand the use of higher–order theories in each of the constitutive layers separately with a accompanying rise in the number of unknowns in the solution process and complexity of the problem. In other words, each single layer is treated as an independent plate and compatibility of displacement components in relation to each interface is then applied as a constraint. In these cases, LW models are attained. Contrary to the ESL theories, the LWT are developed based on the assumption that the displacement field manifests C^0–continuity across the laminate thickness. Therefore, the displacements are continuous across the laminate thickness, however, the derivatives of the displacement components with regard to the thickness coordinate may have discontinuity at several points across the thickness, thereby providing the likelihood of the continuous transverse stresses at the interfaces separating dissimilar material properties. LW displacement fields furnish a substantially more kinematically correct illustration of the cross–sectional warping with regard to the deformation of tick laminates.

The principle of minimum total potential energy and LWT have been employed by Yazdani Sarvestani et al. [128] to investigate the impacts of fiber steering on the hygro–thermal and mechanical buckling loads, natural frequency, bending deformation, and stress distributions of shells and circular plates manufactured by AFP technique. The LWT used in this work allowed each layer of the VAT conical panel, as shown in Fig. 24, to behave as a real 3–D layer able to lead to accurate results, in particular for local quantities such as interlaminar stresses. It is worthwhile emphasizing that the accuracy of the LW model has been improved by subdividing each layer into a finite number of numerical layers. The higher number of subdivision through the thickness, the higher accuracy of the results of the fibre–steered shell will be. The numerical results led to the conclusion that fibre–steering in a composite conical panel has resulted in up to 57% and 44% improvements in the buckling loads and fundamental frequencies, respectively. Viglietti et al. [129] reported that analysis of VAT composites structures based on a LW approach leads to accurate results, however, it demands a higher computational cost. Moreover, although the ESL models are not as accurate as the LWT, they can result in a substantial reduction in the computational cost.

8.3. Carrera's Unified Formulation

CUF [24, 26] is a hierarchical formulation using a compact notation that offers a procedure to determine any structural theories, considering variable kinematic representation by virtue of arbitrary expansions of unknown variables, e.g., displacement or stress components. CUF facilitates to deal with any–order theories by accounting the order as an input of the analysis since the governing equations are given resulting from a few fundamental nuclei (FN), whose form does not depend either on the order of the presented approximations or on the selections made for the base functions through the thickness [130, 25]. The use of CUF makes the assembly of the matrices a trivial procedure, which can be comfortably implemented in computer code. The assembly of the matrix includes four loops on indices i, j, τ and s, and an FN is computed for each combination of these indices, as shown in Fig. 25.

Tornabene et al. [131, 132, 133] studied the static and dynamic analyses of doubly–curved panels reinforced by curvilinear fibers based on CUF with different thickness functions along the three orthogonal curvilinear directions. The implemented theory in these works was entirely general and permitted to investigate doubly–curved shells and panels with variable stiffness. Comparing ESL and LWT within the framework of CUF has revealed that when a soft–core is included in the lamination scheme, the ESL theories turn out to be inappropriate. Indeed, the stiffness variations as a result of a more emphasized fiber curvature make necessary the use of an LWT. A refined beam model based on CUF has been developed by Viglietti et al. [129, 134] to the free vibration analysis of plates and a wing structure with an NACA profile made of VAT composites. It was found that the introduction of curvilinear fibers in a lamina can lead to complex coupling impacts which cannot be detected by the classical theories, accordingly, refined models are demanded.

9. Concluding remarks

The present review has summarized the state–of–the–art and the challenges in the modelling, design, and analysis of VAT composite laminates. Thanks to significant advancement and design flexibility offered by fiber placement technologies, a new class of composite structures made by curvilinear fibre steering has been introduced. Steering fiber paths such that the fiber angle distribution varies spatially revealed a great capacity for load redistribution from the central zones of the panels to their supported edge zones, providing for more than doubling the buckling loads in comparison with the most efficient conventional straight fibre designs.

Despite more than twenty years of the appearance of the TFP technology, few papers have been dedicated to the design and modelling of the VAT composite structures manufactured by TFP. There is still need to conduct more fundamental and robust numerical modelling and optimisation strategies of the fibre–steered composite parts with accompanying TFP experimental investigations. It has been reported that the CTS technique could eliminate the process–induced defects of the AFP and TFP techniques, such as fibre buckling and straightening along the inside and outside of the curved tow path. However, this technique is still immature and few studies, all at Bristol University, have been conducted on the design considerations and simulation of the CTS–manufactured fibre–steered composite. It is worthwhile mentioning that in the process of manufacturing fibre–steered laminates, either using the AFP technique or the CTS process, thickness build–up is inevitable. However, in the stiffness tailoring design of the CTS–manufactured composites, the thickness build–up can be integrated with the thickness fibre steering to create variable–stiffness variable–thickness composite laminates. Furthermore, more research on the experiments, modelling and analysis of VAT composite shells manufactured by filament winding is demanded. Filament winding is a well–established process among the composite manufacturing

processes owing to high precision in fiber positioning, high fiber content, good automation capability, and low void content. However, computational modelling and design as well as experimental works on the VAT composites manufactured by filament winding are still immature.

In this review paper, several fibre angle trajectory methods have been reviewed, including linear and non–linear variation of fibre orientation, constant in–plane curvature, and geodesic path. The crucial manufacturable constraints, which imposes some design restrictions on the VAT composite laminates, may hinder full potential of performance improvements over conventional straight fibre laminates. As a result, most important manufacturing limitations have been explained, which should be incorporated into the modelling and analysis of the composite laminates with arbitrary lay–up configurations. The promising results have been reported by using the tow–drop technique. However, to provide more realistic results, the resin rich areas, created by the individual dropping of tows, should be considered in the failure models. These spots are highly susceptible to damage initiation and propagation. This interesting and challenging topic was investigated merely using continuum damage mechanics while in the future research, other sophisticated approaches, such as cohesive zone models, peridynamics, and phase filed approach, can be employed for modelling fracture and damage of VAT composite laminates. Other interesting point drawn out from this review is that to present a realistic model and analysis, residual thermal stresses arising from the laminate curing process should be incorporated. These residual stresses may have an essential impact on the laminate failure, which are not uniform layer–wise like they are for the case of straight fibre ones. Moreover, it has been concluded that in order to present continuous fiber angle orientations, in recent years IGA formulation based on NURBS has drawn substantial attention. IGA is notably more appropriate for the analysis and design of composites with curvilinear fiber paths compared with FEA, since curvilinear fiber paths can be exactly represented by the IGA owing to the superior characteristics of NURBS including smoothness, high–order continuity, and reduction of total degree–of–freedom.

Referring to Table 1, the overwhelming majority of the reviewed papers have been established based on the CLT and FSDT, which fail both to fulfill the interlaminar transverse shear stress continuity at each interface and to explain the zig–zag effect. In particular, the CLT cannot represent properly mechanical behavior of moderately thick to thick laminated composite plates and shells with curvilinear fibre paths. It has been found that although the ESL models are not as accurate as the LWT, they can result in a substantial reduction in the computational cost. Furthermore, the hierarchical nature of CUF has provided the fidelity of the fibre–steered composite laminate model to be tuned, such that low–fidelity and high–fidelity models can be employed simultaneously to determine global response and 3–D stresses, even when greatly localised.

References

[1] C.-F. Schleussner, T. K. Lissner, E. M. Fischer, J. Wohland, M. Perrette, A. Golly, J. Rogelj, K. Childers, J. Schewe, K. Frieler, et al., Differential climate impacts for policy-relevant limits to global warming: the case of 1.5 c and 2 c, Earth system dynamics 7 (2016) 327–351.

[2] L. Hollaway, Advanced fibre-reinforced polymer (frp) composite materials for sustainable energy technologies, in: Advanced Fibre-Reinforced Polymer (FRP) Composites for Structural Applications, Elsevier, 2013, pp. 737–779.

[3] Z. Gurdal, R. Olmedo, In-plane response of laminates with spatially varying fiber orientations-variable stiffness concept, AIAA journal 31 (4) (1993) 751–758.

[4] R. Kapania, J. Li, H. Kapoor, Optimal design of unitized panels with curvilinear stiffeners, in: AIAA 5th ATIO and16th Lighter-Than-Air Sys Tech. and Balloon Systems Conferences, 2005, p. 7482.

[5] P. Hao, Y. Wang, C. Liu, B. Wang, K. Tian, G. Li, Q. Wang, L. Jiang, Hierarchical non-deterministic optimization of curvilinearly stiffened panel with multicutouts, Aiaa Journal 56 (10) (2018) 4180–4194.

[6] D. Wang, M. M. Abdalla, Z.-P. Wang, Z. Su, Streamline stiffener path optimization (sspo) for embedded stiffener layout design of non-uniform curved grid-stiffened composite (ncgc) structures, Computer Methods in Applied Mechanics and Engineering 344 (2019) 1021–1050.

[7] B. Wang, X. Ma, K. Tian, P. Hao, Y. Zhou, D. Quan, Concurrent patch optimization of hybrid composite plates based on proper orthogonal decomposition, AIAA Journal 57 (11) (2019) 4915–4926.

[8] P. Hao, B. Wang, K. Tian, G. Li, X. Zhang, Optimization of curvilinearly stiffened panels with single cutout concerning the collapse load, International Journal of Structural Stability and Dynamics 16 (07) (2016) 1550036.

[9] P. Hao, B. Wang, K. Tian, G. Li, K. Du, F. Niu, Efficient optimization of cylindrical stiffened shells with reinforced cutouts by curvilinear stiffeners, AIAA Journal 54 (4) (2016) 1350–1363.

[10] P. Hao, D. Liu, K. Zhang, Y. Yuan, B. Wang, G. Li, X. Zhang, Intelligent layout design of curvilinearly stiffened panels via deep learning-based method, Materials & Design 197 (2021) 109180.

[11] H.-J. L. Dirk, C. Ward, K. D. Potter, The engineering aspects of automated prepreg layup: History, present and future, Composites Part B: Engineering 43 (3) (2012) 997–1009.

[12] D. O. Evans, M. M. Vaniglia, P. C. Hopkins, Fiber placement process study, Tomorrow's Materials: Today. 34 (1989) 1822–1833.

[13] F. Bullock, S. Kowalski, R. Young, Automated prepreg tow placement for composite structures., ADVANCED MATERIALS: THE CHALLENGE FOR THE NEXT DECADE. 1 (1990) 734–745.

[14] B. C. Kim, K. Potter, P. M. Weaver, Continuous tow shearing for manufacturing variable angle tow composites, Composites Part A: Applied Science and Manufacturing 43 (8) (2012) 1347–1356.

[15] B. C. Kim, P. M. Weaver, K. Potter, Manufacturing characteristics of the continuous tow shearing method for manufacturing of variable angle tow composites, Composites Part A: Applied Science and Manufacturing 61 (2014) 141–151.

[16] P. Crothers, K. Drechsler, D. Feltin, I. Herszberg, T. Kruckenberg, Tailored fibre placement to minimise stress concentrations, Composites Part A: Applied Science and Manufacturing 28 (7) (1997) 619–625.

[17] P. Mattheij, K. Gliesche, D. Feltin, Tailored fiber placement-mechanical properties and applications, Journal of Reinforced Plastics and Composites 17 (9) (1998) 774–786.

[18] P. Mattheij, K. Gliesche, D. Feltin, 3d reinforced stitched carbon/epoxy laminates made by tailored fibre placement, Composites Part A: Applied Science and Manufacturing 31 (6) (2000) 571–581.

[19] K. Uhlig, L. Bittrich, A. Spickenheuer, J. H. S. Almeida Jr, Waviness and fiber volume content analysis in continuous carbon fiber reinforced plastics made by tailored fiber placement, Composite Structures 222 (2019) 110910.

[20] A. Sawicki, P. Minguett, The effect of intraply overlaps and gaps upon the compression strength of composite laminates, in: 39th AIAA/ASME/ASCE/AHS/ASC Structures, Structural Dynamics, and Materials Conference and Exhibit, 1998, p. 1786.

[21] A. Beakou, M. Cano, J.-B. Le Cam, V. Verney, Modelling slit tape buckling during automated prepreg manufacturing: A local approach, Composite structures 93 (10) (2011) 2628–2635.

[22] K. Croft, L. Lessard, D. Pasini, M. Hojjati, J. Chen, A. Yousefpour, Experimental study of the effect of automated fiber placement induced defects on performance of composite laminates, Composites Part A: Applied Science and Manufacturing 42 (5) (2011) 484–491.

[23] Z. Kazancı, A review on the response of blast loaded laminated composite plates, Progress in Aerospace Sciences 81 (2016) 49–59.

[24] E. Carrera, Theories and finite elements for multilayered plates and shells: a unified compact formulation with numerical assessment and benchmarking, Archives of Computational Methods in Engineering 10 (3) (2003) 215–296.

[25] E. Carrera, S. Brischetto, P. Nali, Plates and shells for smart structures: classical and advanced theories for modeling and analysis, Vol. 36, John Wiley & Sons, 2011.

[26] E. Carrera, M. Cinefra, M. Petrolo, E. Zappino, Finite element analysis of structures through unified formulation, John Wiley & Sons, 2014.

[27] H. Ghiasi, K. Fayazbakhsh, D. Pasini, L. Lessard, Optimum stacking sequence design of composite materials part ii: Variable stiffness design, Composite structures 93 (1) (2010) 1–13.

[28] H. Ghiasi, K. Fayazbakhsh, D. Pasini, L. Lessard, Optimum stacking sequence design of composite materials part ii: Variable stiffness design, Composite structures 93 (1) (2010) 1–13.

[29] P. Ribeiro, H. Akhavan, A. Teter, J. Warmiński, A review on the mechanical behaviour of curvilinear fibre composite laminated panels, Journal of Composite Materials 48 (22) (2014) 2761–2777.

[30] G. G. Lozano, A. Tiwari, C. Turner, S. Astwood, A review on design for manufacture of variable stiffness composite laminates, Proceedings of the Institution of Mechanical Engineers, Part B: Journal of Engineering Manufacture 230 (6) (2016) 981–992.

[31] A. Sabido, L. Bahamonde, R. Harik, M. J. van Tooren, Maturity assessment of the laminate variable stiffness design process, Composite Structures 160 (2017) 804–812.

[32] Z. Xin, Y. Duan, W. Xu, T. Zhang, B. Wang, Review of the mechanical performance of variable stiffness design fiber-reinforced composites, Science and Engineering of Composite Materials 25 (3) (2018) 425–437.

[33] J. Plocher, A. Panesar, Review on design and structural optimisation in additive manufacturing: Towards next-generation lightweight structures, Materials & Design 183 (2019) 108164.

[34] M. Y. Matveev, P. J. Schubel, A. C. Long, I. Jones, Understanding the buckling behaviour of steered tows in automated dry fibre placement (adfp), Composites Part A: Applied Science and Manufacturing 90 (2016) 451–456.

[35] B. Kim, K. Hazra, P. Weaver, K. Potter, Limitations of fibre placement techniques for variable angle tow composites and their process-induced defects, in: Proceedings of the 18th International Conference on Composite Materials (ICMM18), Jeju, Korea, 2011, pp. 21–26.

[36] L. Bittrich, A. Spickenheuer, J. H. S. Almeida, S. Müller, L. Kroll, G. Heinrich, Optimizing variable-axial fiber-reinforced composite laminates: the direct fiber path optimization concept, Mathematical Problems in Engineering 2019.

[37] K. Gliesche, T. Hübner, H. Orawetz, Application of the tailored fibre placement (tfp) process for a local reinforcement on an "open-hole" tension plate from carbon/epoxy laminates, Composites Science and Technology 63 (1) (2003) 81–88.

[38] K. Uhlig, M. Tosch, L. Bittrich, A. Leipprand, S. Dey, A. Spickenheuer, G. Heinrich, Meso-scaled finite element analysis of fiber reinforced plastics made by tailored fiber placement, Composite Structures 143 (2016) 53–62.

[39] Y. Zhu, Y. Qin, S. Qi, H. Xu, D. Liu, C. Yan, Variable angle tow reinforcement design for locally reinforcing an open-hole composite plate, Composite Structures 202 (2018) 162–169.

[40] J. H. S. Almeida Jr, L. Bittrich, A. Spickenheuer, Improving the open-hole tension characteristics with variable-axial composite laminates: Optimization, progressive damage modeling and experimental observations, Composites Science and Technology 185 (2020) 107889.

[41] J. H. S. Almeida Jr, L. Bittrich, E. Jansen, V. Tita, A. Spickenheuer, Buckling optimization of composite cylinders for axial compression: A design methodology considering a variable-axial fiber layout, Composite Structures 222 (2019) 110928.

[42] J. H. S. Almeida Jr, L. Bittrich, T. Nomura, A. Spickenheuer, Cross-section optimization of topologically-optimized variable-axial anisotropic composite structures, Composite Structures 225 (2019) 111150.

[43] E. D. Zympeloudis, Development of a composite tape placement technology with advanced fibre steering capability, Ph.D. thesis, PhD thesis, University of Bristol (2019).

[44] B. C. Kim, P. M. Weaver, K. Potter, Computer aided modelling of variable angle tow composites manufactured by continuous tow shearing, Composite Structures 129 (2015) 256–267.

[45] R. Groh, P. Weaver, Buckling analysis of variable angle tow, variable thickness panels with transverse shear effects, Composite Structures 107 (2014) 482–493.

[46] T. D. Dang, S. R. Hallet, B. C. Kim, Y. L. Cahain, R. Butler, W. Liu, Modelling of as manufactured geometry for prediction of impact and compression after impact behaviour of variable angle tow laminates, Journal of Composite Materials 49 (12) (2015) 1423–1438.

[47] Z. Wu, G. Raju, P. M. Weaver, Optimization of postbuckling behaviour of variable thickness composite panels with variable angle tows: Towards "buckle-free" design concept, International Journal of Solids and Structures 132 (2018) 66–79.

[48] Z. Wu, G. Raju, P. M. Weaver, Framework for the buckling optimization of variable-angle tow composite plates, AIAA Journal 53 (12) (2015) 3788–3804.

[49] D. Peeters, M. Abdalla, Optimization of ply drop locations in variable-stiffness composites, AIAA Journal 54 (5) (2016) 1760–1768.

[50] D. Peeters, Design optimisation of practical variable stiffness and thickness laminates, Ph.D. thesis, PhD Thesis, TU Delft (2017).

[51] C. Waldhart, Analysis of tow-placed, variable-stiffness laminates, Ph.D. thesis, MSc Thesis. Blacksburg, Virginia Tech (1996).

[52] P. Hao, X. Liu, Y. Wang, D. Liu, B. Wang, G. Li, Collaborative design of fiber path and shape for complex composite shells based on isogeometric analysis, Computer Methods in Applied Mechanics and Engineering 354 (2019) 181–212.

[53] L. Parnas, S. Oral, Ü. Ceyhan, Optimum design of composite structures with curved fiber courses, Composites science and technology 63 (7) (2003) 1071–1082.

[54] S. Setoodeh, A. Blom, M. Abdalla, Z. Gürdal, Generating curvilinear fiber paths from lamination parameters distribution, in: 47th AIAA/ASME/ASCE/AHS/ASC Structures, Structural Dynamics, and Materials Conference 14th AIAA/ASME/AHS Adaptive Structures Conference 7th, 2006, p. 1875.

[55] A. Alhajahmad, M. M. Abdalla, Z. Gürdal, Design tailoring for pressure pillowing using tow-placed steered fibers, Journal of Aircraft 45 (2) (2008) 630–640.

[56] A. W. Blom, M. M. Abdalla, Z. Gürdal, Optimization of course locations in fiber-placed panels for general fiber angle distributions, Composites Science and Technology 70 (4) (2010) 564–570.

[57] Z. Wu, P. M. Weaver, G. Raju, B. C. Kim, Buckling analysis and optimisation of variable angle tow composite plates, Thin-walled structures 60 (2012) 163–172.

[58] Z. Wu, P. M. Weaver, G. Raju, Postbuckling optimisation of variable angle tow composite plates, Composite Structures 103 (2013) 34–42.

[59] W. Zhao, R. K. Kapania, Prestressed vibration of stiffened variable-angle tow laminated plates, AIAA Journal 57 (6) (2019) 2575–2593.

[60] D. C. Jegley, B. F. Tatting, Z. Guerdal, Automated finite element analysis of elastically-tailored plates, NASA/CR-2003-212679.

[61] A. W. Blom, C. S. Lopes, P. J. Kromwijk, Z. Gurdal, P. P. Camanho, A theoretical model to study the influence of tow-drop areas on the stiffness and strength of variable-stiffness laminates, Journal of composite materials 43 (5) (2009) 403–425.

[62] J. M. Van Campen, C. Kassapoglou, Z. Gürdal, Generating realistic laminate fiber angle distributions for optimal variable stiffness laminates, Composites Part B: Engineering 43 (2) (2012) 354–360.

[63] O. Falcó, J. Mayugo, C. Lopes, N. Gascons, A. Turon, J. Costa, Variable-stiffness composite panels: As-manufactured modeling and its influence on the failure behavior, Composites Part B: Engineering 56 (2014) 660–669.

[64] M. A. Nik, K. Fayazbakhsh, D. Pasini, L. Lessard, Optimization of variable stiffness composites with embedded defects induced by automated fiber placement, Composite Structures 107 (2014) 160–166.

[65] M. Baruch, J. Arbocz, G. Zhang, Laminated conical shells-considerations for the variations of the stiffness coefficients, in: 35th Structures, Structural Dynamics, and Materials Conference, 1994, p. 1634.

[66] Y. Goldfeld, J. Arbocz, Buckling of laminated conical shells given the variations of the stiffness coefficients, AIAA journal 42 (3) (2004) 642–649.

[67] Y. Goldfeld, J. Arbocz, A. Rothwell, Design and optimization of laminated conical shells for buckling, Thin-Walled Structures 43 (1) (2005) 107–133.

[68] A. W. Blom, S. Setoodeh, J. M. Hol, Z. Gürdal, Design of variable-stiffness conical shells for maximum fundamental eigenfrequency, Computers & structures 86 (9) (2008) 870–878.

[69] A. W. Blom, B. F. Tatting, J. M. Hol, Z. Gürdal, Fiber path definitions for elastically tailored conical shells, Composites part B: engineering 40 (1) (2009) 77–84.

[70] A. W. Blom, Structural performance of fiber-placed, variable-stiffness composite conical and cylindrical shells, Ph.D. thesis, PhD Thesis. TU Delft (2010).

[71] C. J. Brampton, K. C. Wu, H. A. Kim, New optimization method for steered fiber composites using the level set method, Structural and Multidisciplinary Optimization 52 (3) (2015) 493–505.

[72] X.-Y. Zhou, X. Ruan, P. Gosling, Thermal buckling optimization of variable angle tow fibre composite plates with gap/overlap free design, Composite Structures 223 (2019) 110932.

[73] G. G. Lozano, A. Tiwari, C. Turner, A design algorithm to model fibre paths for manufacturing of structurally optimised composite laminates, Composite Structures 204 (2018) 882–895.

[74] K. Fayazbakhsh, M. A. Nik, D. Pasini, L. Lessard, Defect layer method to capture effect of gaps and overlaps in variable stiffness laminates made by automated fiber placement, Composite Structures 97 (2013) 245–251.

[75] S. Nagendra, S. Kodiyalam, J. Davis, V. Parthasarathy, Optimization of tow fiber paths for composite design, in: 36th Structures, Structural Dynamics and Materials Conference, 1995, p. 1275.

[76] V. Mishra, D. M. Peeters, M. M. Abdalla, Stiffness and buckling analysis of variable stiffness laminates including the effect of automated fibre placement defects, Composite Structures 226 (2019) 111233.

[77] B. F. Tatting, Design and manufacture of elastically tailored tow placed plates, National Aeronautics and Space Administration, Langley Research Center, 2002.

[78] C. Wu, Z. Gurdal, J. Starnes, Structural response of compression-loaded, tow-placed, variable stiffness panels, in: 43rd AIAA/ASME/ASCE/AHS/ASC Structures, Structural Dynamics, and Materials Conference, 2002, p. 1512.

[79] O. Falcó, C. Lopes, F. Naya, F. Sket, P. Maimí, J. Mayugo, Modelling and simulation of tow-drop effects arising from the manufacturing of steered-fibre composites, Composites Part A: Applied Science and Manufacturing 93 (2017) 59–71.

[80] S. Setoodeh, M. M. Abdalla, S. T. IJsselmuiden, Z. Gürdal, Design of variable-stiffness composite panels for maximum buckling load, Composite structures 87 (1) (2009) 109–117.

[81] S. Setoodeh, M. M. Abdalla, Z. Gürdal, Design of variable–stiffness laminates using lamination parameters, Composites Part B: Engineering 37 (4-5) (2006) 301–309.

[82] E. Demir, P. Yousefi-Louyeh, M. Yildiz, Design of variable stiffness composite structures using lamination parameters with fiber steering constraint, Composites Part B: Engineering 165 (2019) 733–746.

[83] T. Shafighfard, E. Demir, M. Yildiz, Design of fiber-reinforced variable-stiffness composites for different open-hole geometries with fiber continuity and curvature constraints, Composite Structures 226 (2019) 111280.

[84] P. Hao, X. Yuan, C. Liu, B. Wang, H. Liu, G. Li, F. Niu, An integrated framework of exact modeling, isogeometric analysis and optimization for variable-stiffness composite panels, Computer Methods in Applied Mechanics and Engineering 339 (2018) 205–238.

[85] P. Hao, X. Yuan, H. Liu, B. Wang, C. Liu, D. Yang, S. Zhan, Isogeometric buckling analysis of composite variable-stiffness panels, Composite Structures 165 (2017) 192–208.

[86] V. Khalafi, J. Fazilati, Parametric instability behavior of tow steered laminated quadrilateral plates using isogeometric analysis, Thin-Walled Structures 133 (2018) 96–105.

[87] J. Fazilati, V. Khalafi, Aeroelastic panel flutter optimization of tow-steered variable stiffness composite laminated plates using isogeometric analysis, Journal of Reinforced Plastics and Composites 38 (19-20) (2019) 885–895.

[88] E. Shafei, S. Faroughi, T. Rabczuk, Multi-patch nurbs formulation for anisotropic variable angle tow composite plates, Composite Structures 241 (2020) 111964.

[89] F. Heinecke, C. Willberg, Manufacturing-induced imperfections in composite parts manufactured via automated fiber placement, Journal of Composites Science 3 (2) (2019) 56.

[90] M. Y. Matveev, F. G. Ball, I. A. Jones, A. C. Long, P. J. Schubel, M. Tretyakov, Uncertainty in geometry of fibre preforms manufactured with automated dry fibre placement and its effects on permeability, Journal of Composite Materials 52 (16) (2018) 2255–2269.

[91] X.-Y. Zhou, P. Gosling, Towards an understanding of variations in the buckling of tailored variable angle tow composite plates, Composite Structures 203 (2018) 797–809.

[92] M. Walker, R. Hamilton, A technique for optimally designing fibre-reinforced laminated plates with manufacturing uncertainties for maximum buckling strength, Engineering Optimization 37 (2) (2005) 135–144.

[93] X.-Y. Zhou, X. Ruan, P. Gosling, Robust design optimization of variable angle tow composite plates for maximum buckling load in the presence of uncertainties, Composite Structures 223 (2019) 110985.

[94] P. Hao, Y. Wang, R. Ma, H. Liu, B. Wang, G. Li, A new reliability-based design optimization framework using isogeometric analysis, Computer Methods in Applied Mechanics and Engineering 345 (2019) 476–501.

[95] Z. Wang, J. H. S. Almeida Jr, L. St-Pierre, Z. Wang, S. G. Castro, Reliability-based buckling optimization with an accelerated kriging metamodel for filament-wound variable angle tow composite cylinders, Composite Structures 254 (2020) 112821.

[96] J. N. Reddy, Mechanics of laminated composite plates and shells: theory and analysis, CRC press, 2003.

[97] E. Carrera, Theories and finite elements for multilayered, anisotropic, composite plates and shells, Archives of Computational Methods in Engineering 9 (2) (2002) 87–140.

[98] E. Carrera, Cz requirements—models for the two dimensional analysis of multilayered structures, Composite structures 37 (3-4) (1997) 373–383.

[99] Z. Guerdal, R. Olmedo, Composite laminates with spatially varying fiber orientations-'variable stiffness panel concept', in: 33rd Structures, Structural Dynamics and Materials Conference, 1992, p. 2472.

[100] Z. Wu, G. Raju, P. M. Weaver, Postbuckling analysis of variable angle tow composite plates, International Journal of Solids and Structures 50 (10) (2013) 1770–1780.

[101] O. Stodieck, J. E. Cooper, P. M. Weaver, P. Kealy, Improved aeroelastic tailoring using tow-steered composites, Composite Structures 106 (2013) 703–715.

[102] R. Groh, P. M. Weaver, S. White, G. Raju, Z. Wu, A 2d equivalent single-layer formulation for the effect of transverse shear on laminated plates with curvilinear fibres, Composite Structures 100 (2013) 464–478.

[103] M. Yas, B. S. Aragh, Elasticity solution for free vibration analysis of four-parameter functionally graded fiber orientation cylindrical panels using differential quadrature method, European Journal of Mechanics-A/Solids 30 (5) (2011) 631–638.

[104] B. Sobhaniaragh, M. Nejati, W. Mansur, Buckling modelling of ring and stringer stiffened cylindrical shells aggregated by graded cnts, Composites Part B: Engineering 124 (2017) 120–133.

[105] B. Sobhaniaragh, R. Batra, W. Mansur, F. Peters, Thermal response of ceramic matrix nanocomposite cylindrical shells using eshelby-mori-tanaka homogenization scheme, Composites Part B: Engineering 118 (2017) 41–53.

[106] J. Reddy, Simple finite elements with relaxed continuity for nonlinear analysis of plates, Finite element methods in engineering (1980) 265–281.

[107] J. N. Reddy, Energy and variational methods in applied mechanics: with an introduction to the finite element method, Wiley New York, 1984.

[108] R. Vescovini, E. Spigarolo, E. Jansen, L. Dozio, Efficient post-buckling analysis of variable-stiffness plates using a perturbation approach, Thin-Walled Structures 143 (2019) 106211.

[109] K. Liang, Q. Sun, Y. Zhang, Nonlinear buckling analysis of variable stiffness composite plates based on the reduced order model, Composite Structures 206 (2018) 681–692.

[110] A. Khani, M. M. Abdalla, Z. Gürdal, Circumferential stiffness tailoring of general cross section cylinders for maximum buckling load with strength constraints, Composite Structures 94 (9) (2012) 2851–2860.

[111] X. Chen, Z. Wu, G. Nie, P. Weaver, Buckling analysis of variable angle tow composite plates with a through-the-width or an embedded rectangular delamination, International Journal of Solids and Structures 138 (2018) 166–180.

[112] G. Raju, Z. Wu, B. C. Kim, P. M. Weaver, Prebuckling and buckling analysis of variable angle tow plates with general boundary conditions, Composite Structures 94 (9) (2012) 2961–2970.

[113] E. Reissner, On bending of elastic plates, Quarterly of Applied Mathematics 5 (1) (1947) 55–68.

[114] H. Hencky, Über die berücksichtigung der schubverzerrung in ebenen platten, ingenieur-archiv 16 (1) (1947) 72–76.

[115] R. Mindlin, Influence of rotatory inertia and shear on flexural motions of isotropic, elastic plates, J. appl. Mech. 18 (1951) 31–38.

[116] C. M. Wang, G. Lim, J. Reddy, K. Lee, Relationships between bending solutions of reissner and mindlin plate theories, Engineering structures 23 (7) (2001) 838–849.

[117] H.-T. Thai, S.-E. Kim, A review of theories for the modeling and analysis of functionally graded plates and shells, Composite Structures 128 (2015) 70–86.

[118] A. M. Antunes, P. Ribeiro, J. D. Rodrigues, H. Akhavan, Modal analysis of a variable stiffness composite laminated plate with diverse boundary conditions: experiments and modelling, Composite Structures 239 (2020) 111974.

[119] J. Whitney, C. Sun, A higher order theory for extensional motion of laminated composites, Journal of Sound and Vibration 30 (1) (1973) 85–97.

[120] K. H. Lo, R. M. Christensen, E. M. Wu, A high-order theory of plate deformation—part 1: Homogeneous plates, Journal of Applied Mechanics 44 (4) (1977) 663–668.

[121] T. Kant, Numerical analysis of thick plates, Computer methods in Applied Mechanics and engineering 31 (1) (1982) 1–18.

[122] A. Bhimaraddi, L. K. Stevens, A higher order theory for free vibration of orthotropic, homogeneous, and laminated rectangular plates, Journal of Applied Mechanics 51 (1) (1984) 195–198.

[123] N. Hanna, A. Leissa, A higher order shear deformation theory for the vibration of thick plates, Journal of Sound and Vibration 170 (4) (1994) 545–555.

[124] J. Reddy, A refined nonlinear theory of plates with transverse shear deformation, International Journal of solids and structures 20 (9-10) (1984) 881–896.

[125] S. J. Mehrabadi, B. S. Aragh, On the thermal analysis of 2-d temperature-dependent functionally graded open cylindrical shells, Composite Structures 96 (2013) 773–785.

[126] M. Levinson, An accurate, simple theory of the statics and dynamics of elastic plates, MECH. RES. COMMUN. 7 (6) (1980) 343–350.

[127] A. Akbarzadeh, M. A. Nik, D. Pasini, The role of shear deformation in laminated plates with curvilinear fiber paths and embedded defects, Composite Structures 118 (2014) 217–227.

[128] H. Y. Sarvestani, A. Akbarzadeh, M. Hojjati, Hygro-thermo-mechanical analysis of fiber-steered composite conical panels, Composite Structures 179 (2017) 146–160.

[129] A. Viglietti, E. Zappino, E. Carrera, Analysis of variable angle tow composites structures using variable kinematic models, Composites Part B: Engineering 171 (2019) 272–283.

[130] E. Carrera, G. Giunta, M. Petrolo, Beam structures: classical and advanced theories, John Wiley & Sons, 2011.

[131] F. Tornabene, N. Fantuzzi, M. Bacciocchi, E. Viola, Higher-order theories for the free vibrations of doubly-curved laminated panels with curvilinear reinforcing fibers by means of a local version of the gdq method, Composites Part B: Engineering 81 (2015) 196–230.

[132] F. Tornabene, N. Fantuzzi, M. Bacciocchi, Higher-order structural theories for the static analysis of doubly-curved laminated composite panels reinforced by curvilinear fibers, Thin-Walled Structures 102 (2016) 222–245.

[133] F. Tornabene, N. Fantuzzi, M. Bacciocchi, Foam core composite sandwich plates and shells with variable stiffness: Effect of the curvilinear fiber path on the modal response, Journal of Sandwich Structures & Materials 21 (1) (2019) 320–365.

[134] A. Viglietti, E. Zappino, E. Carrera, Free vibration analysis of variable angle-tow composite wing structures, Aerospace Science and Technology 92 (2019) 114–125.

[135] M. M. Abdalla, S. Setoodeh, Z. Gürdal, Design of variable stiffness composite panels for maximum fundamental frequency using lamination parameters, Composite structures 81 (2) (2007) 283–291.

[136] Z. Gürdal, B. F. Tatting, C. Wu, Variable stiffness composite panels: effects of stiffness variation on the in-plane and buckling response, Composites Part A: Applied Science and Manufacturing 39 (5) (2008) 911–922.

[137] A. W. Blom, P. B. Stickler, Z. Gürdal, Optimization of a composite cylinder under bending by tailoring stiffness properties in circumferential direction, Composites Part B: Engineering 41 (2) (2010) 157–165.

[138] A. Khani, S. T. IJsselmuiden, M. M. Abdalla, Z. Gürdal, Design of variable stiffness panels for maximum strength using lamination parameters, Composites Part B: Engineering 42 (3) (2011) 546–552.

[139] H. Haddadpour, Z. Zamani, Curvilinear fiber optimization tools for aeroelastic design of composite wings, Journal of Fluids and Structures 33 (2012) 180–190.

[140] M. A. Nik, K. Fayazbakhsh, D. Pasini, L. Lessard, Surrogate-based multi-objective optimization of a composite laminate with curvilinear fibers, Composite Structures 94 (8) (2012) 2306–2313.

[141] T. D. Dang, S. R. Hallett, A numerical study on impact and compression after impact behaviour of variable angle tow laminates, Composite Structures 96 (2013) 194–206.

[142] M. Rouhi, H. Ghayoor, S. V. Hoa, M. Hojjati, Effect of structural parameters on design of variable-stiffness composite cylinders made by fiber steering, Composite Structures 118 (2014) 472–481.

[143] S. C. White, G. Raju, P. M. Weaver, Initial post-buckling of variable-stiffness curved panels, Journal of the Mechanics and Physics of Solids 71 (2014) 132–155.

[144] S. C. White, Post-buckling of variable-stiffness shell structures, Ph.D. thesis, PhD thesis, University of Bristol (2016).

[145] M. A. Nik, K. Fayazbakhsh, D. Pasini, L. Lessard, A comparative study of metamodeling methods for the design optimization of variable stiffness composites, Composite Structures 107 (2014) 494–501.

[146] M. A. Nik, L. Lessard, D. Pasini, Size-dependent behavior of laminates with curvilinear fibers made by automated fiber placement, Science and Engineering of Composite Materials 22 (2) (2015) 157–163.

[147] R. Butler, Buckling and compressive strength of laminates with optimized fibre-steering and layer-stacking for aerospace applications, in: Polymer composites in the aerospace industry, Elsevier, 2015, pp. 77–97.

[148] A. Venkatachari, S. Natarajan, M. Ganapathi, M. Haboussi, Mechanical buckling of curvilinear fibre composite laminate with material discontinuities and environmental effects, Composite Structures 131 (2015) 790–798.

[149] A. Duran, N. Fasanella, V. Sundararaghavan, A. Waas, Thermal buckling of composite plates with spatial varying fiber orientations, Composite Structures 124 (2015) 228–235.

[150] B. H. Coburn, P. M. Weaver, Buckling analysis, design and optimisation of variable-stiffness sandwich panels, International journal of solids and structures 96 (2016) 217–228.

[151] A. Madeo, R. Groh, G. Zucco, P. Weaver, G. Zagari, R. Zinno, Post-buckling analysis of variable-angle tow composite plates using koiter's approach and the finite element method, Thin-Walled Structures 110 (2017) 1–13.

[152] M. Loja, J. Barbosa, C. M. Soares, Dynamic instability of variable stiffness composite plates, Composite Structures 182 (2017) 402–411.

[153] D. Peeters, Z. Hong, M. Abdalla, A compliance approximation method applied to variable stiffness composite optimisation, Structural and Multidisciplinary Optimization 58 (5) (2018) 1981–2001.

[154] Y. Tian, S. Pu, Z. Zong, T. Shi, Q. Xia, Optimization of variable stiffness laminates with gap-overlap and curvature constraints, Composite Structures 230 (2019) 111494.

[155] P. Hao, D. Liu, Y. Wang, X. Liu, B. Wang, G. Li, S. Feng, Design of manufacturable fiber path for variable-stiffness panels based on lamination parameters, Composite Structures 219 (2019) 158–169.

[156] A. Haldar, R. Groh, E. Jansen, P. M. Weaver, R. Rolfes, An efficient semi-analytical framework to tailor snap-through loads in bistable variable stiffness laminates, International Journal of Solids and Structures.

[157] Z. Zamani, H. Haddadpour, M.-R. Ghazavi, Curvilinear fiber optimization tools for design thin walled beams, Thin-Walled Structures 49 (3) (2011) 448–454.

[158] P. Ribeiro, Non-linear free periodic vibrations of variable stiffness composite laminated plates, Nonlinear Dynamics 70 (2) (2012) 1535–1548.

[159] P. Ribeiro, H. Akhavan, Non-linear vibrations of variable stiffness composite laminated plates, Composite Structures 94 (8) (2012) 2424–2432.

[160] G. Huang, H. Wang, G. Li, An efficient reanalysis assisted optimization for variable-stiffness composite design by using path functions, Composite Structures 153 (2016) 409–420.

[161] M. G. Günay, T. Timarci, Static analysis of thin-walled laminated composite closed-section beams with variable stiffness, Composite Structures 182 (2017) 67–78.

[162] P. Hao, C. Liu, X. Liu, X. Yuan, B. Wang, G. Li, M. Dong, L. Chen, Isogeometric analysis and design of variable-stiffness aircraft panels with multiple cutouts by level set method, Composite Structures 206 (2018) 888–902.

[163] M. Rasool, M. Singha, Stability behavior of variable stiffness composite panels under periodic in-plane shear and compression, Composites Part B: Engineering 172 (2019) 472–484.

[164] M. Rasool, M. Singha, Stability of variable stiffness composite laminates under compressive and shearing follower forces, Composite Structures 225 (2019) 111003.

[165] F. S. Liguori, G. Zucco, A. Madeo, D. Magisano, L. Leonetti, G. Garcea, P. M. Weaver, Postbuckling optimisation of a variable angle tow composite wingbox using a multi-modal koiter approach, Thin-Walled Structures 138 (2019) 183–198.

[166] J. Fazilati, V. Khalafi, Effects of embedded perforation geometry on the free vibration of tow-steered variable stiffness composite laminated panels, Thin-Walled Structures 144 (2019) 106287.

[167] M. Montemurro, A. Catapano, A general b-spline surfaces theoretical framework for optimisation of variable angle-tow laminates, Composite Structures 209 (2019) 561–578.

[168] S. G. Castro, M. V. Donadon, T. A. Guimarães, Es-pim applied to buckling of variable angle tow laminates, Composite Structures 209 (2019) 67–78.

[169] T. Farsadi, D. Asadi, H. Kurtaran, Nonlinear flutter response of a composite plate applying curvilinear fiber paths, Acta Mechanica 231 (2) (2020) 715–731.

[170] C. S. Lopes, P. P. Camanho, Z. Gürdal, B. F. Tatting, Progressive failure analysis of tow-placed, variable-stiffness composite panels, International Journal of Solids and Structures 44 (25-26) (2007) 8493–8516.

[171] C. Lopes, Z. Gürdal, P. Camanho, Variable-stiffness composite panels: Buckling and first-ply failure improvements over straight-fibre laminates, Computers & Structures 86 (9) (2008) 897–907.

[172] C. S. Lopes, Damage and failure of non-conventional composite laminates, Ph.D. thesis, PhD Thesis, TU Delft (2009).

[173] C. S. Lopes, Z. Gürdal, P. Camanho, Tailoring for strength of composite steered-fibre panels with cutouts, Composites Part A: Applied Science and Manufacturing 41 (12) (2010) 1760–1767.

[174] H. Akhavan, P. Ribeiro, Natural modes of vibration of variable stiffness composite laminates with curvilinear fibers, Composite Structures 93 (11) (2011) 3040–3047.

[175] H. Akhavan, P. Ribeiro, M. De Moura, Large deflection and stresses in variable stiffness composite laminates with curvilinear fibres, International Journal of Mechanical Sciences 73 (2013) 14–26.

[176] V. S. Gomes, C. S. Lopes, F. F. A. Pires, Z. Gürdal, P. P. Camanho, Fibre steering for shear-loaded composite panels with cutouts, Journal of Composite Materials 48 (16) (2014) 1917–1926.

[177] A. Venkatachari, S. Natarajan, K. Ramajeyathilagam, M. Ganapathi, Assessment of certain higher-order structural models based on global approach for bending analysis of curvilinear composite laminates, Composite Structures 118 (2014) 548–559.

[178] H. Akhavan, P. Ribeiro, M. F. de Moura, Damage onset on tow-placed variable stiffness composite laminates, Composite Structures 113 (2014) 419–428.

[179] M. Rouhi, H. Ghayoor, S. V. Hoa, M. Hojjati, Multi-objective design optimization of variable stiffness composite cylinders, Composites Part B: Engineering 69 (2015) 249–255.

[180] S. C. White, P. M. Weaver, K. C. Wu, Post-buckling analyses of variable-stiffness composite cylinders in axial compression, Composite Structures 123 (2015) 190–203.

[181] A. Tullu, B.-S. Kang, Elastic deformation of fiber-reinforced multi-layered composite cylindrical shells of variable stiffness, Composites Part B: Engineering 100 (2016) 44–55.

[182] A. Akbarzadeh, M. A. Nik, D. Pasini, Vibration responses and suppression of variable stiffness laminates with optimally steered fibers and magnetostrictive layers, Composites Part B: Engineering 91 (2016) 315–326.

[183] F. Ye, H. Wang, G. Li, Variable stiffness composite material design by using support vector regression assisted efficient global optimization method, Structural and Multidisciplinary Optimization 56 (1) (2017) 203–219.

[184] H. Ghayoor, M. Rouhi, S. V. Hoa, M. Hojjati, Use of curvilinear fibers for improved bending-induced buckling capacity of elliptical composite cylinders, International Journal of Solids and Structures 109 (2017) 112–122.

[185] A. Venkatachari, S. Natarajan, M. Ganapathi, Variable stiffness laminated composite shells–free vibration characteristics based on higher-order structural theory, Composite Structures 188 (2018) 407–414.

[186] M. Rouhi, H. Ghayoor, J. Fortin-Simpson, T. T. Zacchia, S. V. Hoa, M. Hojjati, Design, manufacturing, and testing of a variable stiffness composite cylinder, Composite Structures 184 (2018) 146–152.

[187] D. M. Peeters, G. G. Lozano, M. M. Abdalla, Effect of steering limit constraints on the performance of variable stiffness laminates, Computers & Structures 196 (2018) 94–111.

[188] P. Anilkumar, A. Haldar, E. Jansen, B. Rao, R. Rolfes, Design optimization of multistable variable-stiffness laminates, Mechanics of Advanced Materials and Structures 26 (1) (2019) 48–55.

[189] D. A. Narayan, M. Ganapathi, B. Pradyumna, M. Haboussi, Investigation of thermo-elastic buckling of variable stiffness laminated composite shells using finite element approach based on higher-order theory, Composite Structures 211 (2019) 24–40.

[190] S. Yazdani, P. Ribeiro, Geometrically non-linear static analysis of unsymmetric composite plates with curvilinear fibres: p-version layerwise approach, Composite Structures 118 (2014) 74–85.

[191] S. Yazdani, P. Ribeiro, A layerwise p-version finite element formulation for free vibration analysis of thick composite laminates with curvilinear fibres, Composite Structures 120 (2015) 531–542.

[192] L. Demasi, G. Biagini, F. Vannucci, E. Santarpia, R. Cavallaro, Equivalent single layer, zig-zag, and layer wise theories for variable angle tow composites based on the generalized unified formulation, Composite Structures 177 (2017) 54–79.

[193] M. Patni, S. Minera, R. Groh, A. Pirrera, P. Weaver, On the accuracy of localised 3d stress fields in tow-steered laminated composite structures, Composite Structures 225 (2019) 111034.

[194] A. Spickenheuer, M. Schulz, K. Gliesche, G. Heinrich, Using tailored fibre placement technology for stress adapted design of composite structures, Plastics, rubber and composites 37 (5) (2008) 227–232.

Table 1: Summary of the literature reviewed on the modelling, design, and analysis of the VAT composite structures.

Structural plate & shell theory	Ref. (Year)	Structural objective	Analysis	Manufacturing constraint	Reference path definition
CLT	[3] (1993)	Stress distribution	Closed–form solutions	–	LVFO
	[60] (2003)	Max. buckling load	FEM (STAGS–A)	Gaps and overlaps	LVFO
	[66] (2004)	Buckling behavior	FEM (STAGS–A)	–	GP
	[81] (2006)	Min. compliance	FEM	–	LVFO
	[135] (2007)	Optimal natural frequency	FEM	–	LVFO
	[136] (2008)	Buckling behavior	Rayleigh–Ritz method	–	LVFO
	[80] (2009)	Max. buckling load	FEM	Smoothness of fiber paths	LVFO
	[56] (2010)	Minimizing max. ply thickness, Maximizing surface smoothness	FEM	Gaps and overlaps, Ply staggering	NVFO
	[137] (2010)	Max. buckling load,	FEM	Effective course width, Amount of fibre steering	CIC
	[138] (2011)	Max. strength	FEM	–	LVFO
	[112] (2012)	Pre–buckling and buckling behavior	GDQM	–	LVFO
	[110] (2012)	Max. buckling load	Finite difference method	Minimum turning radius	LVFO
	[57] (2012)	Pre–buckling loads distributions, Max. buckling load	Rayleigh–Ritz method	–	NVFO
	[139] (2012)	Max. aeroelastic instability	Extended Galerkin method	–	LVFO
	[140] (2012)	Max. buckling load and stiffness	Closed–form solutions	–	LVFO
	[100] (2013)	Post–buckling behavior	Rayleigh–Ritz method	–	LVFO
	[101] (2013)	Aeroelastic behaviour	Rayleigh–Ritz method	–	LVFO
	[58] (2013)	Max. post–buckling performance	Rayleigh–Ritz method	–	NVFO
	[141] (2013)	Impact and post–impact compression	FEM	–	LVFO
	[142] (2014)	Max. buckling load	FEM	–	LVFO
	[143] (2014), [144] (2016)	Initial post–buckling response	GDQ+GIQ	–	LVFO
	[145] (2014)	Max. buckling load	FEM	–	LVFO
	[64] (2014), [146] (2015)	Max. buckling load and stiffness	Closed–form solutions	Minimum turning radius, Gaps and overlaps	CIC
	[147] (2015)	Max. buckling load	Closed–form solutions	–	LVFO
	[148] (2015)	Buckling characteristics	FEM	–	LVFO
	[149] (2015)	Thermal buckling resistance	Galerkin method	–	LVFO
	[150] (2016)	Buckling behavior	Ritz energy method	–	LVFO
	[151] (2017)	Post–buckling behavior	GDQM	–	LVFO
	[152] (2017)	Dynamic stability	Rayleigh–Ritz method	Minimum turning radius	LVFO
	[153] (2018)	Min. compliance	FEM	Fibre continuity, Minimum turning radius	LVFO
	[47] (2018)	Buckle–Free design	Rayleigh–Ritz method	Fibre angle deviation Smoothness of fiber paths	NVFO
	[109] (2018)	Max. buckling performance	FEM	–	LVFO
	[108] (2019)	Post–buckling behaviour	Perturbation approach	–	LVFO
	[82] (2019)	Min. compliance	FEM	Minimum turning radius	LVFO
	[154] (2019)	Min. compliance	FEM	Smoothness of fiber paths, Minimum turning radius Gaps and overlaps	LVFO
	[87] (2019)	Flutter stability	IGA	Minimum turning radius	LVFO
	[83] (2019)	Min. compliance	FEM	Continuity of fibers, Minimum turning radius	LVFO
	[155] (2019)	Max. buckling load	IGA	Fibre continuity, Fibre angle deviation, Minimum turning radius	LVFO
	[59] (2019)	Pre–stressed vibration response	FEM	–	NVFO
	[156] (2020)	Snap–through behavior	GDQM	–	NVFO

Table 1: Continued.

Structural plate & shell theory	Ref. (Year)	Structural objective	Analysis	Manufacturing constraint	Reference path definition
FSDT	[53] (2003)	Min. weight	FEM	–	BC
	[157] (2011)	Max. failure load	Extended Galerkin method	Minimum turning radius	LVFO
	[158] (2012)	Free vibration behaviour	FEM	–	LVFO
	[159] (2012)	Linear and non–linear oscillations	FEM	–	LVFO
	[102] (2013)	Flexural behaviour	GDQM	–	LVFO
	[45] (2014)	Buckling behaviour	GDQM	Fibre angle deviation	LVFO
	[160] (2016)	Buckling behaviour	FEM	Minimum turning radius, Fibre angle deviation	LVFO
	[161] (2017)	Flexural–torsional behavior	FEM	–	LVFO
	[85] (2017)	Buckling behaviour	IGA	Continuity of fibers	LVFO
	[111] (2018)	Buckling behaviour	Rayleigh–Ritz method	–	LVFO
	[86] (2018)	Dynamic stability	IGA	–	LVFO
	[162] (2018)	Buckling behaviour	IGA	Minimum turning radius	LVFO
	[163] (2019), [164] (2019)	Stability behavior	FEM	–	LVFO
	[165] (2019)	Buckling and post–buckling behaviour	FEM	Minimum turning radius	LVFO
	[72] (2019)	Thermal buckling performance	FEM	–	LSM
	[166] (2019)	Free vibration characteristics	IGA	–	LVFO
	[52] (2019)	Linear buckling behaviour	IGA	Minimum turning radius	LVFO
	[167] (2019)	Min. compliance	FEM	Minimum turning radius	BSM
	[168] (2019)	Buckling behaviour	Meshless method	–	LVFO
	[169] (2020)	Aeroelastic performance	GDQM	–	LVFO
HSDT	[170] (2007), [171] (2008), [172] (2009)	Stress concentrations around cut–out, Buckling, Progressive damage and failure	FEM (ABAQUS)	Gaps and overlaps, Ply staggering	LVFO
	[68] (2008)	Max. fundamental frequency	FEM (ABAQUS)	Minimum turning radius	LVFO, GP, CIC
	[173] (2010)	Stress concentrations around cut–out, Buckling and post–buckling	FEM (ABAQUS)	Gaps and overlaps, Ply staggering	LVFO
	[174] (2011)	Natural frequencies and mode shapes	FEM	Minimum turning radius	LVFO
	[175] (2013)	Deflection and stresses	FEM	Minimum turning radius	LVFO
	[176] (2014)	Stress concentrations around cut–out, Critical shear buckling load, Post–buckling behaviour	FEM (ABAQUS)	–	LVFO
	[177] (2014)	Static response	FEM	–	LVFO
	[178] (2014)	Deflections and damage onset	FEM	–	LVFO
	[179] (2015)	Max. buckling load	FEM (ABAQUS)	–	LVFO
	[180] (2015)	Buckling and post–buckling behavior	FEM (ABAQUS)	–	LVFO
	[181] (2016)	Strain and stress distributions	FEM (ABAQUS)	Minimum turning radius	LVFO, GP, CIC
	[182] (2016), [127] (2014)	Max. frequency, Static bending & buckling behaviour	Fourier–Galerkin method	Gaps and overlaps	CIC
	[183] (2017)	Max. buckling load	FEM (ABAQUS)	–	LVFO
	[184] (2017)	Max. bending–induced buckling	FEM (ABAQUS)	–	LVFO
	[79] (2017), [63] (2014)	Mechanical behaviour, Failure behavior,	FEM	Gaps and overlaps, Ply staggering, Minimum turning radius	CIC
	[185] (2018)	Free vibration characteristics	FEM	–	LVFO
	[186] (2018)	Max. buckling load	FEM (ABAQUS)	–	LVFO
	[187] (2018)	Max. buckling load	FEM	Gaps and overlaps, Smoothness of fiber paths, Minimum turning radius Number of tows & tow width	LVFO
	[188] (2019)	Snap–through & snap–back behaviors	FEM (ABAQUS)	–	LVFO
	[189] (2019)	Thermo–elastic buckling behavior	FEM	–	LVFO
	[88] (2020)	Dynamic instability	IGA	–	NVFO

Table 1: Continued.

Structural plate & shell theory	Ref. (Year)	Structural objective	Analysis	Manufacturing constraint	Reference path definition
LWT	[190] (2014)	Deflections and stresses distributions	FEM	–	LVFO
	[191] (2015)	Free vibrational behaviour	FEM	–	LVFO
CUF	[132] (2016)	Linear static response	GDQM	–	LVFO
	[192] (2017)	Stress distributions	FEM	–	LVFO
	[134] (2019), [129] (2019)	Free vibration behaviour	FEM	–	LVFO
	[133] (2019)	Natural frequencies	GDQM	–	LVFO
	[193] (2019)	Accurate 3–D stress fields	FEM	–	LVFO

List of Figures

1 Different segments constituting a VAT composite laminated structure along with relevant manufacturing constraints and design considerations. 38

2 **a)**: Total number of publications and citations in the research field of modelling, design, analysis, and manufacturing of VAT composite laminates, **b)**: Geographical distribution of the research works in the research field by country (data from Scopus, as of February 2021). 38

3 Fundamental principle of the TFP method. Adapted with permission from Spickenheuer et al. [194]. 39

4 Tow deformation based on embroidery TFP method; **a)**: Ideal case, **b)**: Real case. Adapted with permission from Kim et al. [35]. 39

5 Three rows of representative unit cells (RUC), while different layers are visible. All layers are shown in the half model (detail left). The stitching yarn is shown only in this demonstration but is considered as resin material in the simulation. On the right the RUC is graphically embedded in the textile preform during the stitching process. Reproduced with permission from Uhlig et al. [38]. 39

6 Buckling modes for cylinders with stacking sequence of: **a)** [0/45/45/0], **b)** [VAT$_s$/45/45/VAT$_s$]. Adapted with permission from Almeida et al. [41]. 40

7 Fibre steering using: **a)** AFP based on in–plane bending deformation, **b)** CTS based on in–plane shear deformation. Reproduced with permission from Kim et al. al. [14]. 40

8 Difference tow arrangement of VAT composites using ; **a)**: AFP technique (tow–drop method), **b)**: CTS technique. Adapted with permission from Kim et al. [14]. 40

9 Thickness change of tow element owing to in–plane shear deformation based on the CTS technique. The tow element with cross–section A–A demonstrates tow thickness before shear while B–B demonstrates the thickness change after shear. . 41

10 CT scan image (top and cross–section views) of a CTS–manufactured VAT composite laminate. Reproduced with permission from Kim et al. [15]. 41

11 Different definitions of reference path based on; **a)**: Linear variation of fibre orientation, **b)**: Constant in–plane curvature. Reproduced from Falco et al. [63]. . . 42

12 Non–linear variation of fiber orientation angles over the VAT plate domain. Reproduced from Wu et al. [57]. 42

13 Conical shell geometry used for the definition of a geodesic path. Reproduced with permission from Blom et al. [68]. 43

14 Comparison of the definition of the fibre angle trajectory based on the geodesic path with those based on the constant angle and constant curvature paths. **a)**: Paths on the 3–D conical shell, **b)**: Paths on the flattened cone. Adapted with permission from Blom [70]. 43

15 Possible issues by ignoring MCL. 44

16 AFP steering path strategies; **a)**: Parallel technique, **b)**: Shifted technique. 44

17 Examples of AFP–manufactured VAT composite panels via; **a)**: Tow–overlap technique, **b)**: Tow–drop technique. Adapted with permission from Lopes et al. [171]. 45

18 Finite element mesh generation of a VAT laminate;**a)**: Non–conforming mesh, **b)**: Tow–drop modeling of the fiber–free zones with structured mesh approach, **c)**: fiber–free zones in a regular mesh domain. Reproduced with permission from Falco et al. [63]. 45

19 Two key approaches for cutting strategy of fibre tows; **a)**: Single–sided strategy, **b)**: Zipper strategy. Adapted with permission from Mishra et al. [76]. 46

20 Tow–drop method with different coverage parameters. 46

21 **a)**: Specimen geometry. **b)**: Tow-drop gap defects (100% gap coverage, 0% gap coverage and 0% gap coverage with staggering). The discontinuity interface in the ply (51–39) is shown using a red line and resin rich zones are shaded in red. **c)**: Tow–drop specimen lay–up with and without staggering. Reproduced with permission from Falco et al. [79]. 47
22 Optimized fiber orientation angle distributions of a VAT plate; **a)**: before and **b)**: after the application of LSC method. Reproduced with permission from Demir et al. [82]. 47
23 Comparison of fiber path modeling for fibre–steered composite panels based on IGA and FEA. Adapted with permission from Hao et al. [84]. 48
24 Schematic representative of coordinate system and ply sequence of an N–layer fiber–steered composite conical panel. Reproduced with permission from Yazdani Sarvestani et al. [128]. 48
25 Assembly procedure used in CUF; the FN is the core, the loops on τ and s establish the matrix for a given pair of i and j, the loops on i and j make the matrix of the elements, and the loop on the elements yield the global stiffness matrix. 49

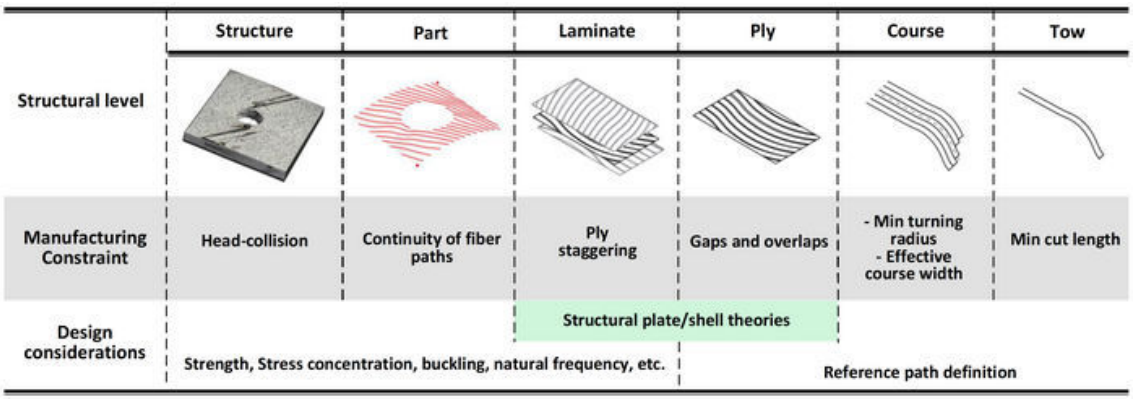
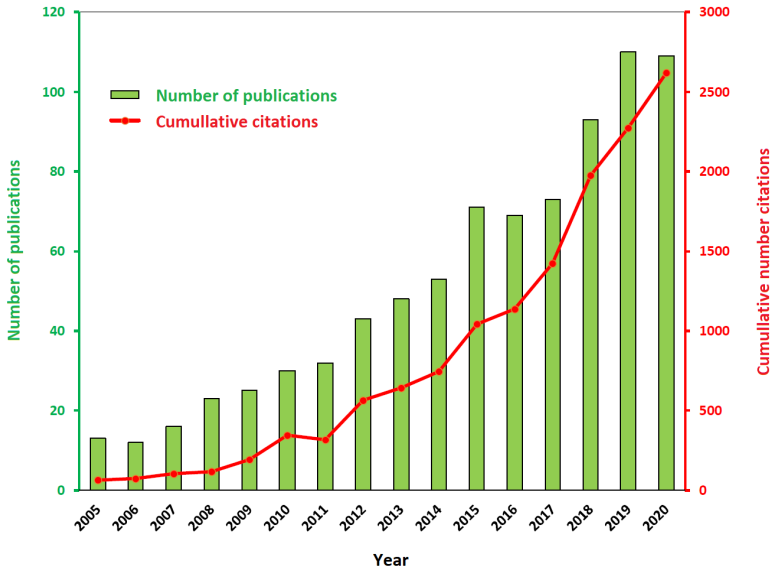
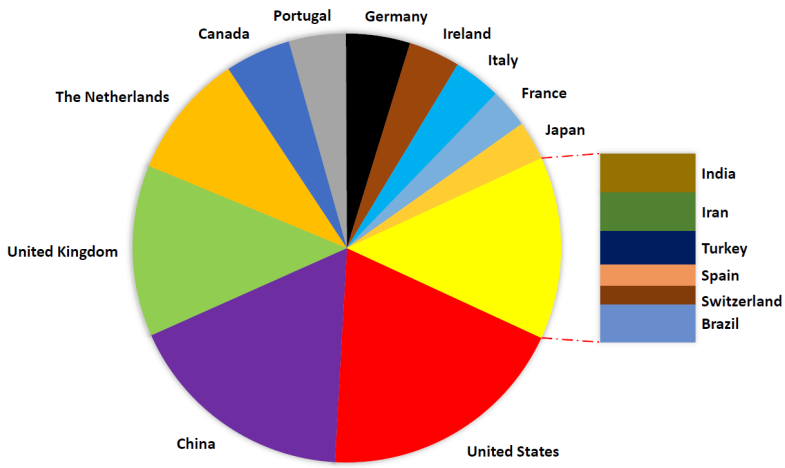


Figure 1: Different segments constituting a VAT composite laminated structure along with relevant manufacturing constraints and design considerations.



(a)



(b)

Figure 2: **a)**: Total number of publications and citations in the research field of modelling, design, analysis, and manufacturing of VAT composite laminates, **b)**: Geographical distribution of the research works in the research field by country (data from Scopus, as of February 2021).

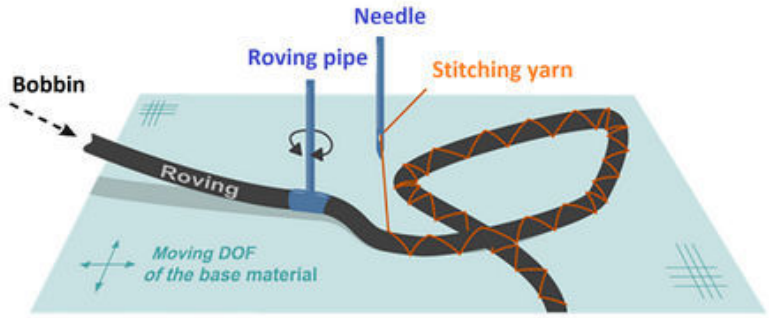


Figure 3: Fundamental principle of the TFP method. Adapted with permission from Spickenheuer et al. [194].

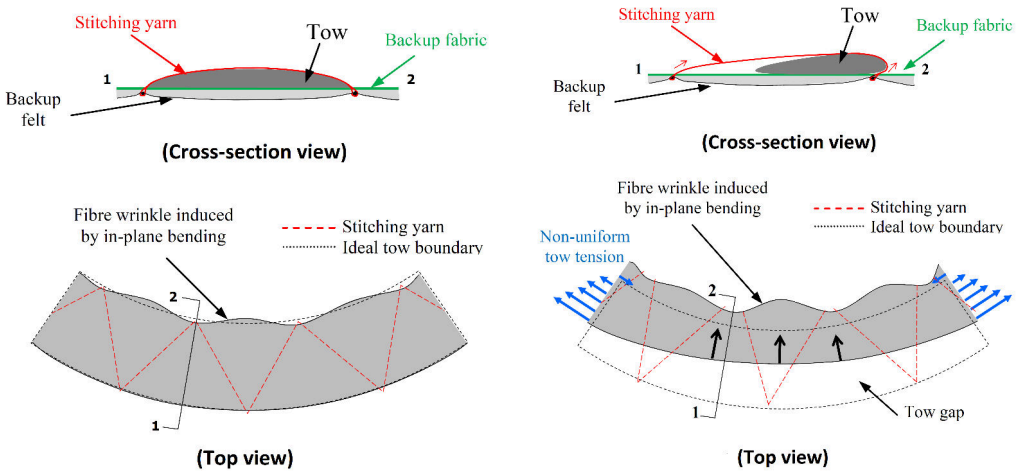


Figure 4: Tow deformation based on embroidery TFP method; **a)**: Ideal case, **b)**: Real case. Adapted with permission from Kim et al. [35].

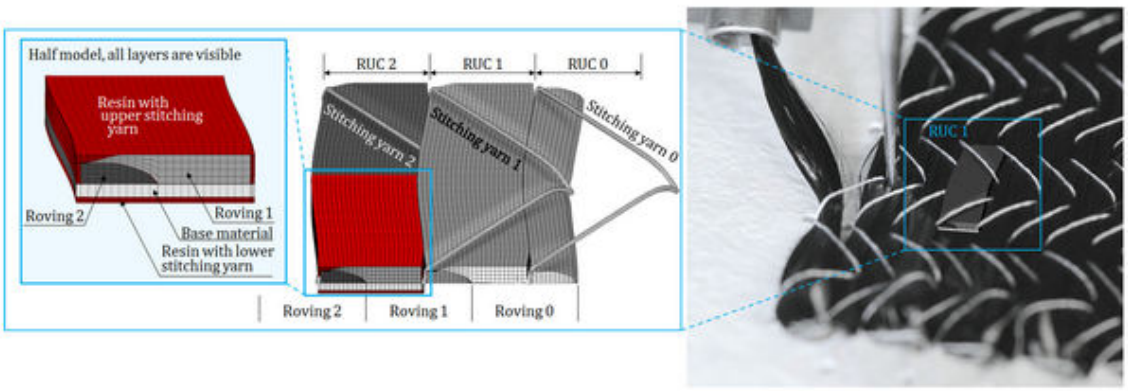


Figure 5: Three rows of representative unit cells (RUC), while different layers are visible. All layers are shown in the half model (detail left). The stitching yarn is shown only in this demonstration but is considered as resin material in the simulation. On the right the RUC is graphically embedded in the textile preform during the stitching process. Reproduced with permission from Uhlig et al. [38].

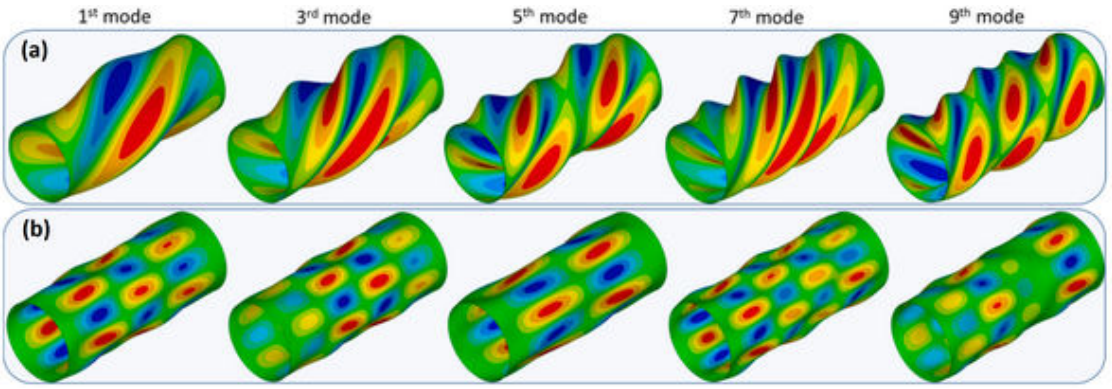


Figure 6: Buckling modes for cylinders with stacking sequence of: **a)** [0/45/45/0], **b)** [VAT$_s$/45/45/VAT$_s$]. Adapted with permission from Almeida et al. [41].

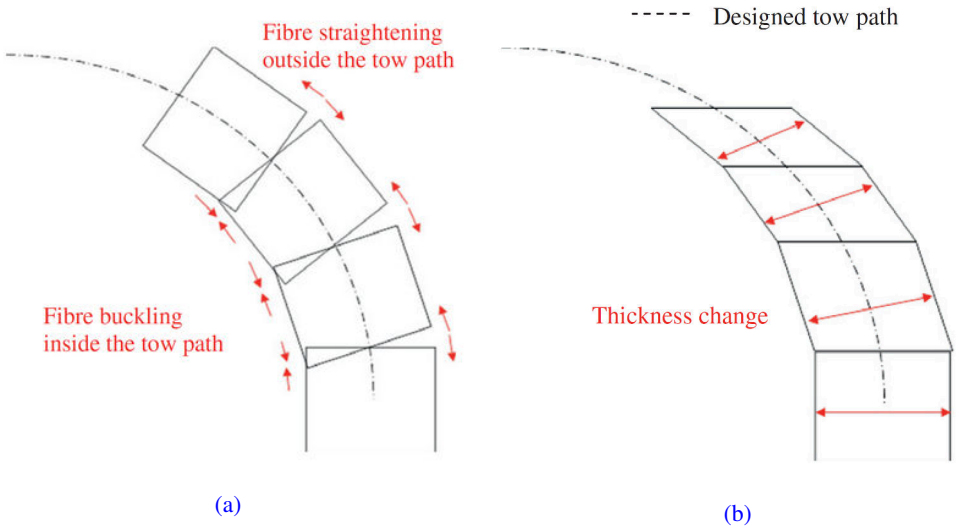


Figure 7: Fibre steering using: **a)** AFP based on in–plane bending deformation, **b)** CTS based on in–plane shear deformation. Reproduced with permission from Kim et al. al. [14].

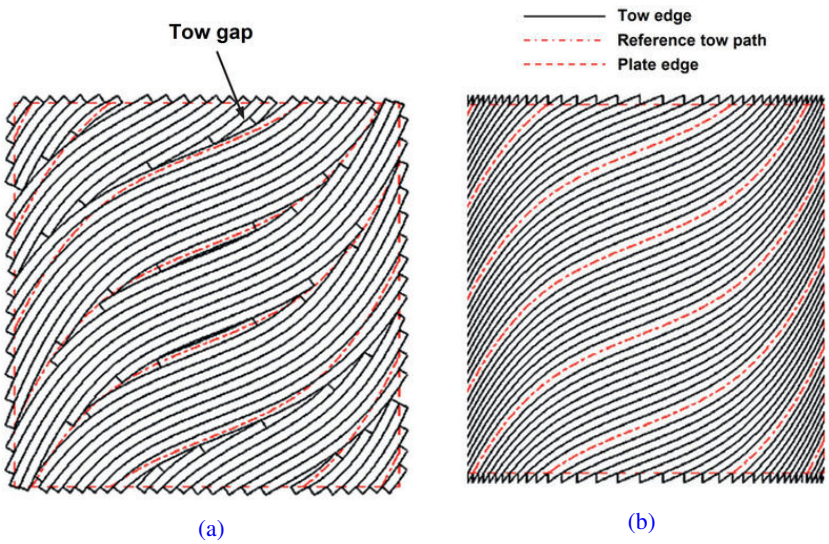


Figure 8: Difference tow arrangement of VAT composites using ; **a)**: AFP technique (tow–drop method), **b)**: CTS technique. Adapted with permission from Kim et al. [14].

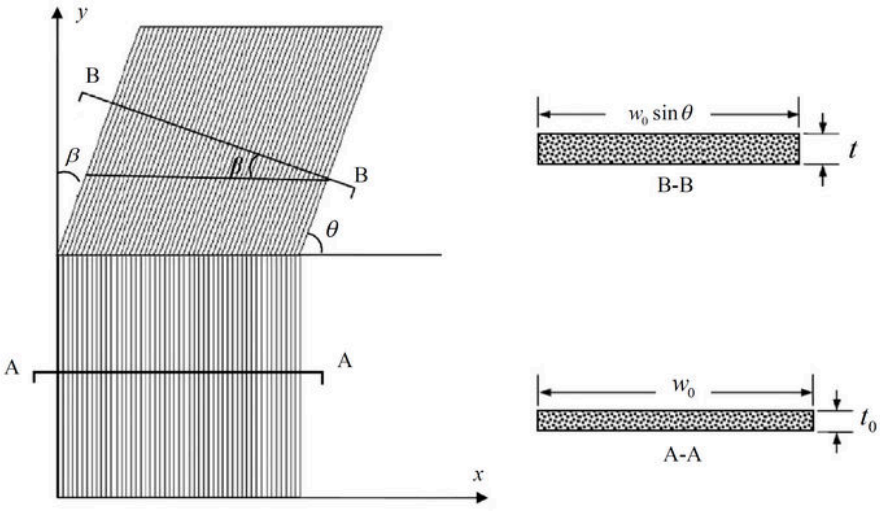


Figure 9: Thickness change of tow element owing to in–plane shear deformation based on the CTS technique. The tow element with cross–section A–A demonstrates tow thickness before shear while B–B demonstrates the thickness change after shear.

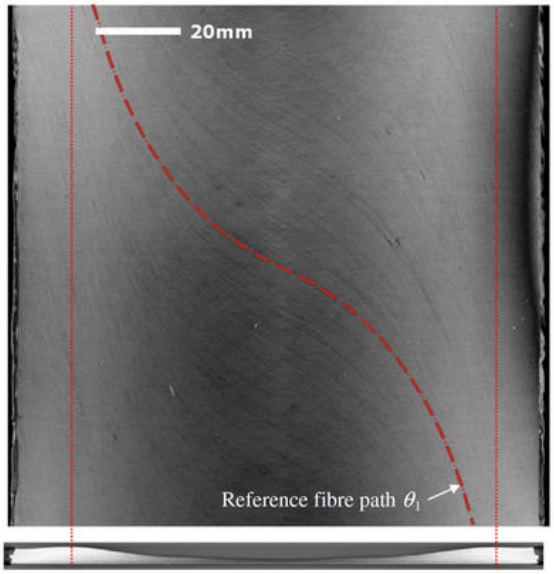


Figure 10: CT scan image (top and cross–section views) of a CTS–manufactured VAT composite laminate. Reproduced with permission from Kim et al. [15].

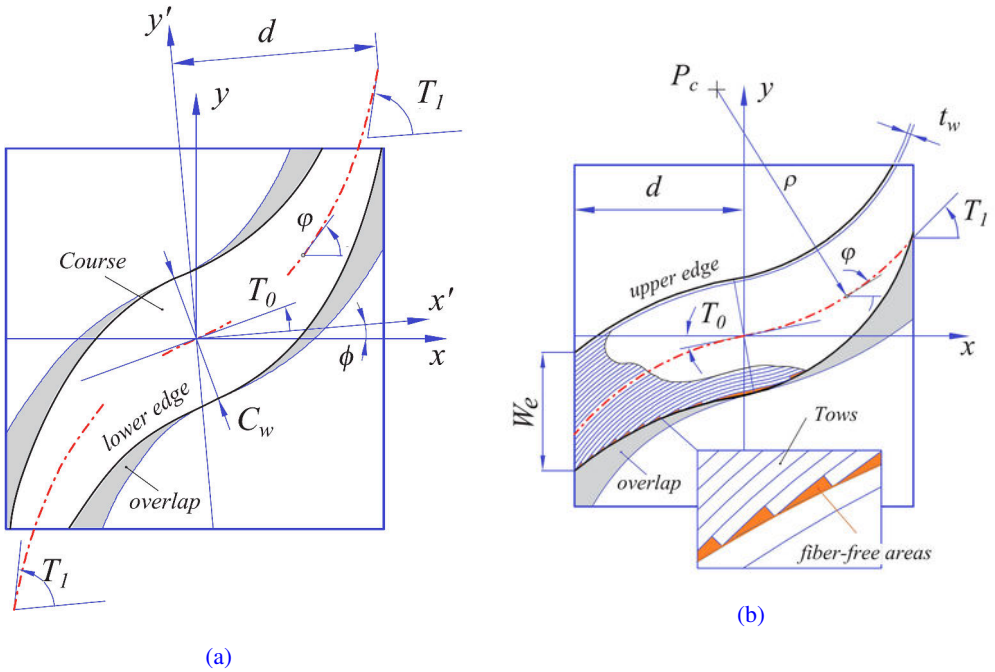


Figure 11: Different definitions of reference path based on; **a)**: Linear variation of fibre orientation, **b)**: Constant in–plane curvature. Reproduced from Falco et al. [63].

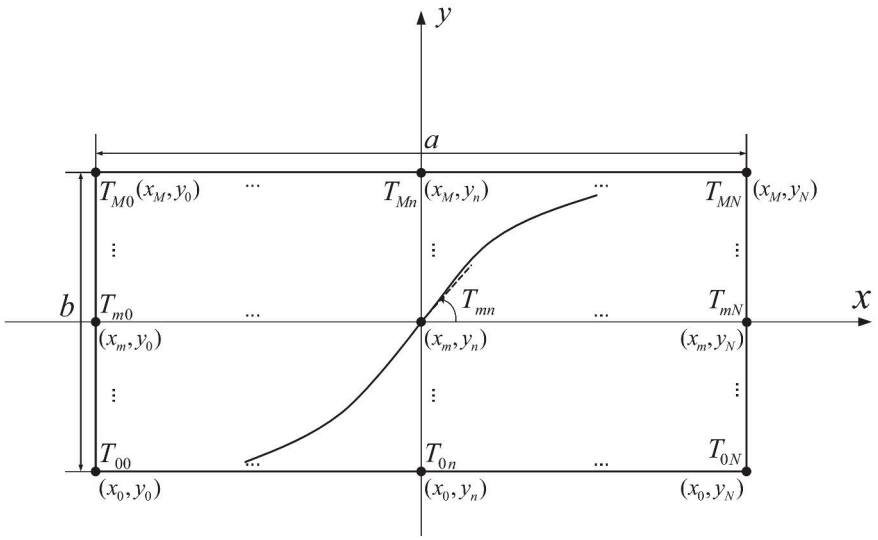


Figure 12: Non–linear variation of fiber orientation angles over the VAT plate domain. Reproduced from Wu et al. [57].

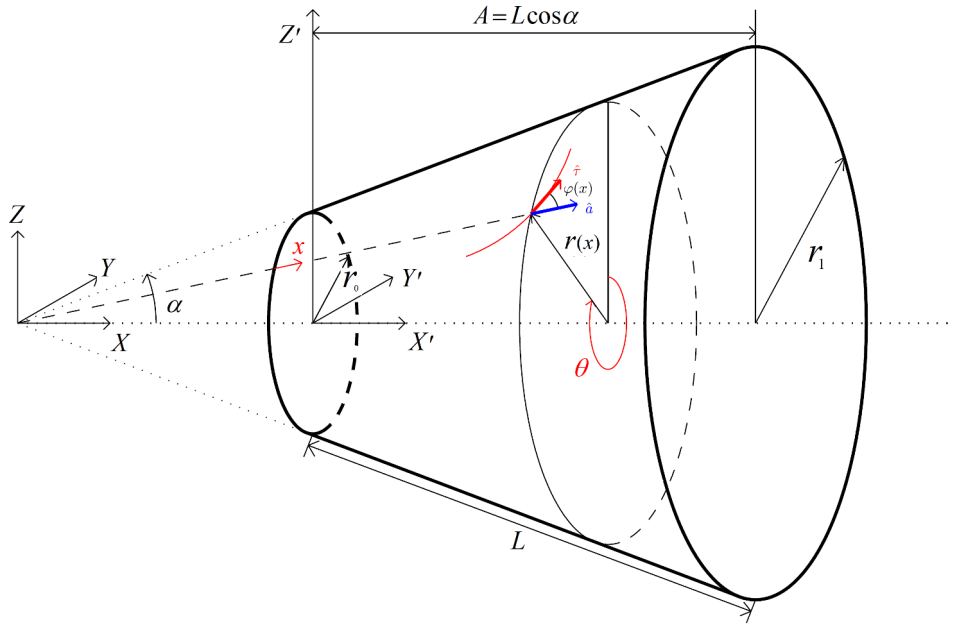


Figure 13: Conical shell geometry used for the definition of a geodesic path. Reproduced with permission from Blom et al. [68].

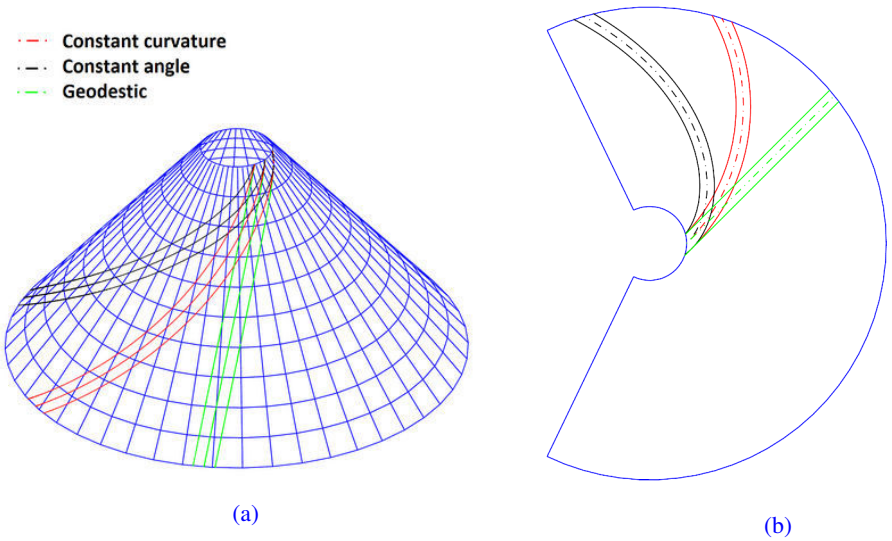


Figure 14: Comparison of the definition of the fibre angle trajectory based on the geodesic path with those based on the constant angle and constant curvature paths. **a)**: Paths on the 3–D conical shell, **b)**: Paths on the flattened cone. Adapted with permission from Blom [70].

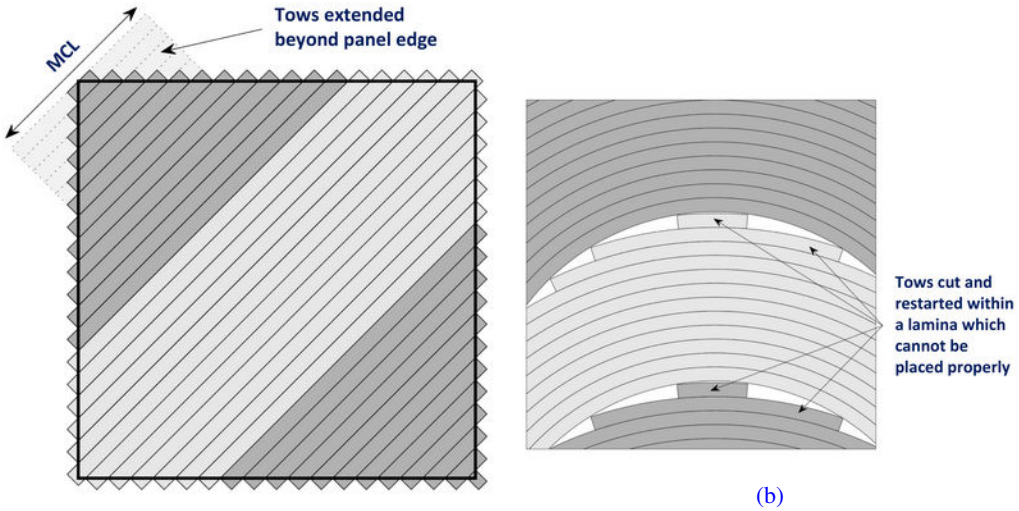


Figure 15: Possible issues by ignoring MCL.

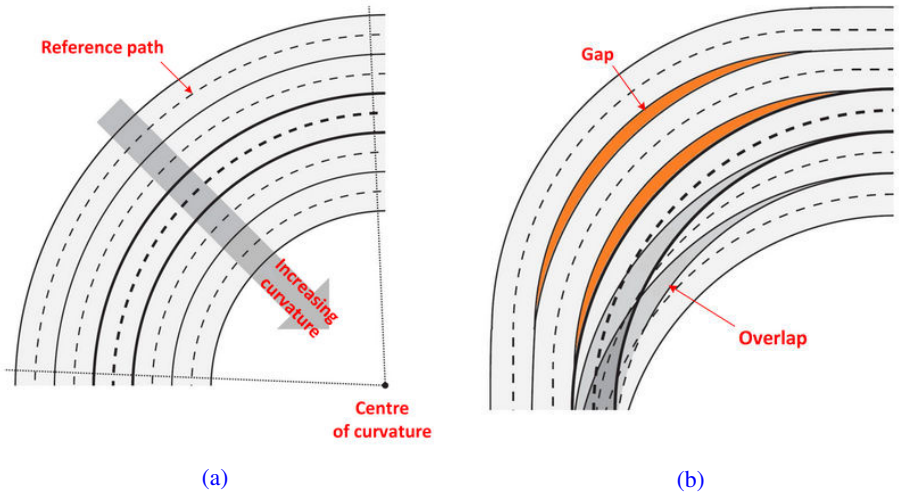
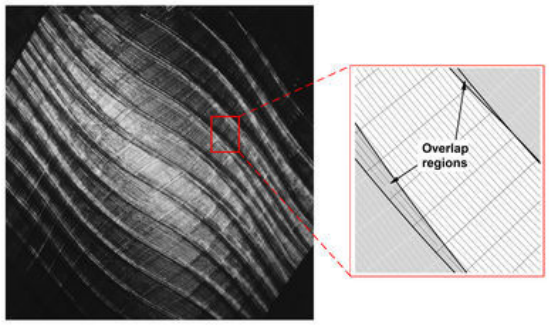
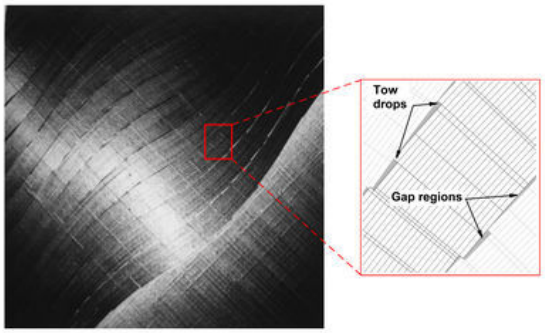


Figure 16: AFP steering path strategies; **a)**: Parallel technique, **b)**: Shifted technique.



(a)



(b)

Figure 17: Examples of AFP–manufactured VAT composite panels via; **a)**: Tow–overlap technique, **b)**: Tow–drop technique. Adapted with permission from Lopes et al. [171].

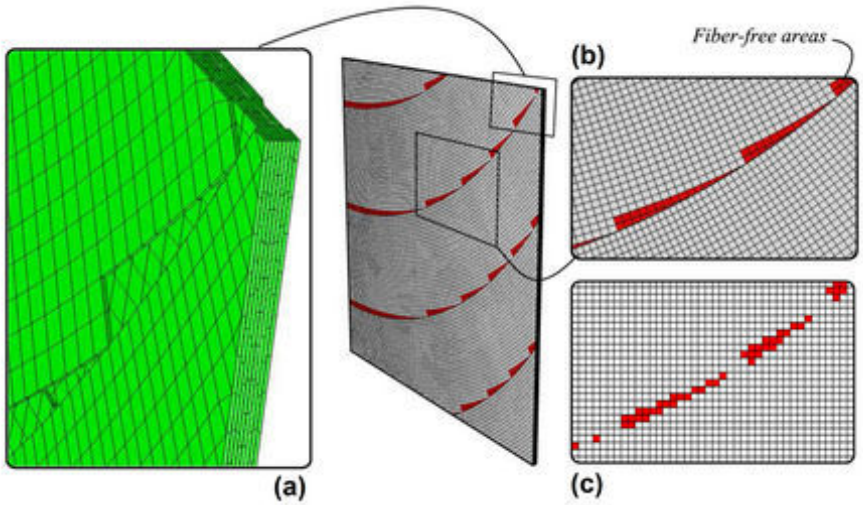


Figure 18: Finite element mesh generation of a VAT laminate;**a)**: Non–conforming mesh, **b)**: Tow–drop modeling of the fiber–free zones with structured mesh approach, **c)**: fiber–free zones in a regular mesh domain. Reproduced with permission from Falco et al. [63].

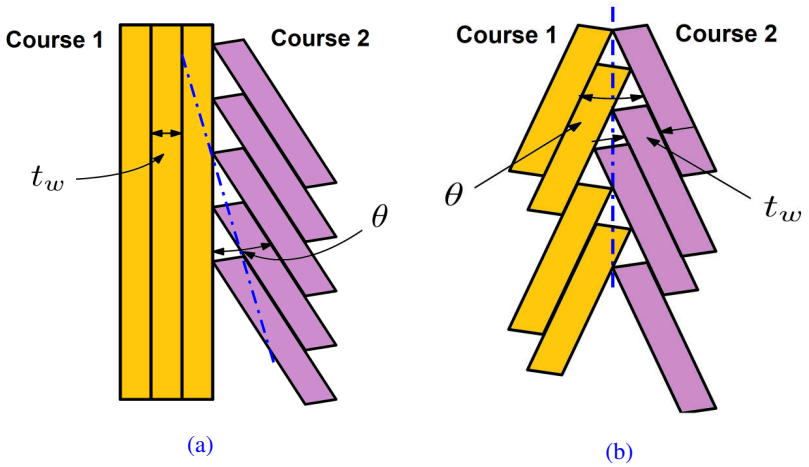


Figure 19: Two key approaches for cutting strategy of fibre tows; **a)**: Single–sided strategy, **b)**: Zipper strategy. Adapted with permission from Mishra et al. [76].

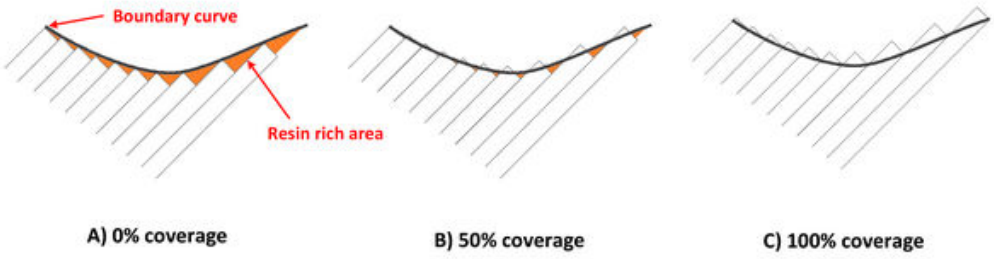


Figure 20: Tow–drop method with different coverage parameters.

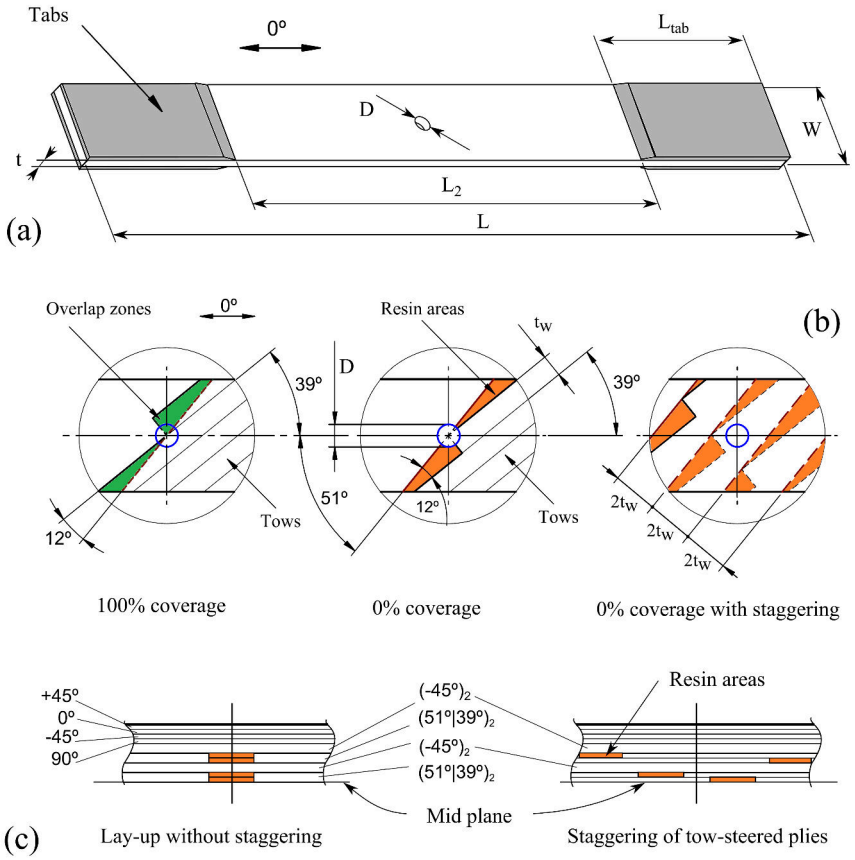
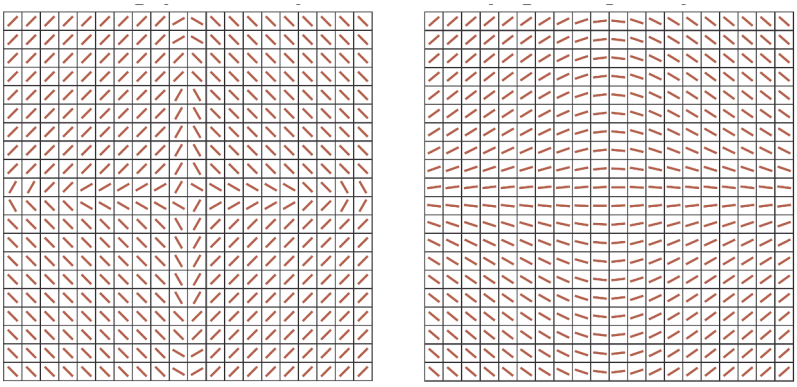


Figure 21: **a)**: Specimen geometry. **b)**: Tow-drop gap defects (100% gap coverage, 0% gap coverage and 0% gap coverage with staggering). The discontinuity interface in the ply (51–39) is shown using a red line and resin rich zones are shaded in red. **c)**: Tow–drop specimen lay–up with and without staggering. Reproduced with permission from Falco et al. [79].



(a) (b)

Figure 22: Optimized fiber orientation angle distributions of a VAT plate; **a)**: before and **b)**: after the application of LSC method. Reproduced with permission from Demir et al. [82].

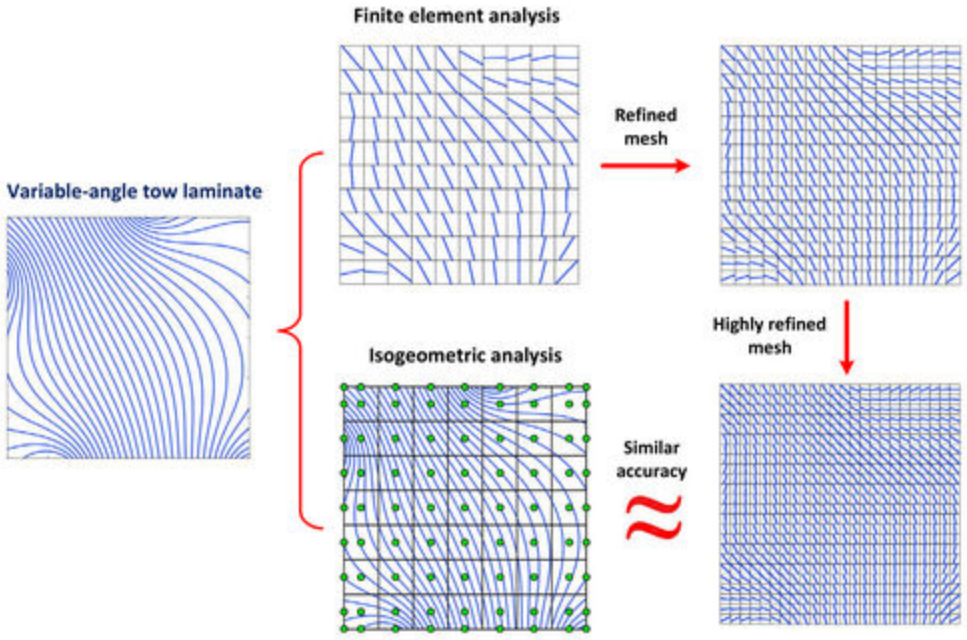


Figure 23: Comparison of fiber path modeling for fibre–steered composite panels based on IGA and FEA. Adapted with permission from Hao et al. [84].

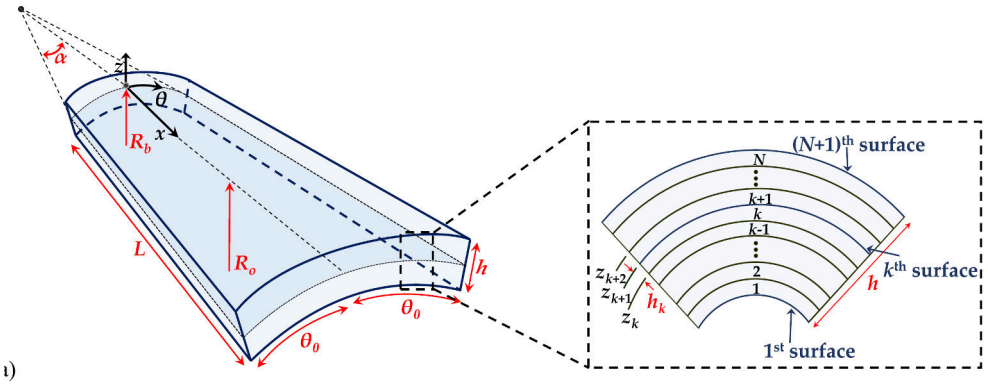


Figure 24: Schematic representative of coordinate system and ply sequence of an N–layer fiber–steered composite conical panel. Reproduced with permission from Yazdani Sarvestani et al. [128].

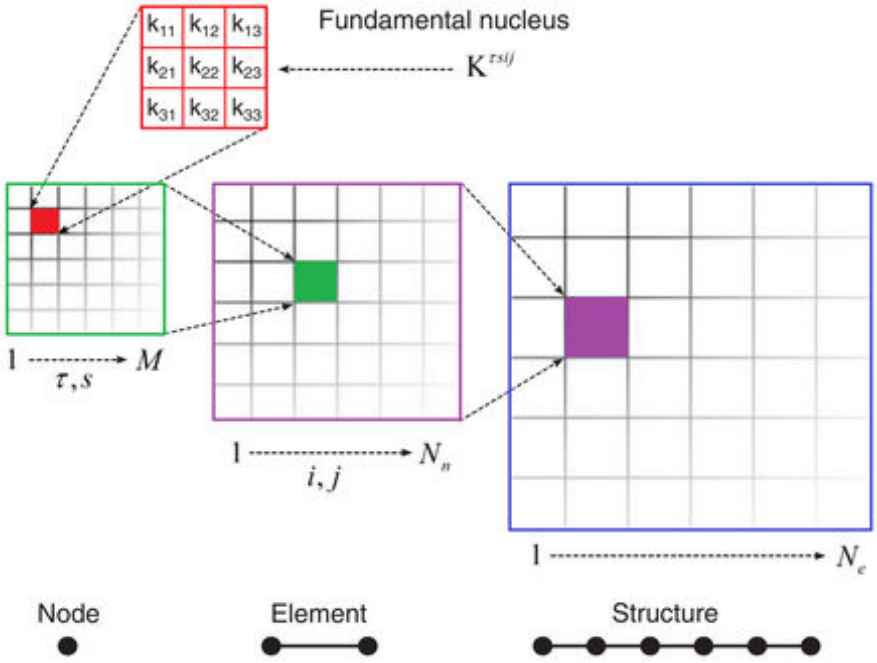


Figure 25: Assembly procedure used in CUF; the FN is the core, the loops on τ and s establish the matrix for a given pair of i and j, the loops on i and j make the matrix of the elements, and the loop on the elements yield the global stiffness matrix.



https://dspace.org/

Manufacturable insight into modelling and design considerations in fibre-steered composite laminates: state of the art and perspective

Aragh, B. Sobhani; Farahani, E. Borzabadi; Xu, B. X.; Ghasemnejad, Hessam; Mansur, W. J.

2021-03-18
Elsevier
https://doi.org/10.1016/j.cma.2021.113752
Sobhani Aragh B, Borzabadi Farahani E, Xu BX, et al., (2021) Manufacturable insight into modelling and design considerations in fibre-steered composite laminates: state of the art and perspective. Computer Methods in Applied Mechanics and Engineering, Volume 379, June 2021, Article number 113752

Downloaded from a DSpace repository. https://dspace.org/